Myelin regulatory factor drives remyelination in multiple sclerosis

Acta Neuropathologica

Myelin Regulatory Factor Drives Remyelination in Multiple Sclerosis

--Manuscript Draft--

Manuscript Number:	ANEU-D-17-00179R2
Full Title:	Myelin Regulatory Factor Drives Remyelination in Multiple Sclerosis
Article Type:	Original Paper
Keywords:	Remyelination; multiple sclerosis; MYRF; oligodendrocyte; Cre-loxP.
Corresponding Author:	Wolfram Tetzlaff University of British Columbia Vancouver, British Columbia CANADA
Corresponding Author Secondary Information:	
Corresponding Author's Institution:	University of British Columbia
Corresponding Author's Secondary Institution:	
First Author:	Greg J. Duncan
First Author Secondary Information:	
Order of Authors:	Greg J. Duncan
	Jason R. Plemel
	Peggy Assinck
	Sohrab B. Manesh
	Fraser G.W. Muir
	Ryan Hirata
	Matan Berson
	Jie Liu
	Michael Wegner
	Ben Emery
	G.R. Wayne Moore
	Wolfram Tetzlaff
Order of Authors Secondary Information:	

Funding Information:	Multiple Sclerosis Society of Canada (EGID 1763)	Dr. Wolfram Tetzlaff
	Multiple Sclerosis Society of Canada (2295)	Prof G.R. Wayne Moore
	Deutsche Forschungsgemeinschaft (We1326/11)	Prof. Michael Wegner
	National Multiple Sclerosis Society (RG5106A1/1)	Dr. Ben Emery
	Canadian Institutes of Health Research (MOP-130475)	Dr. Wolfram Tetzlaff
	Multiple Sclerosis Society of Canada (EGID 2810)	Dr. Wolfram Tetzlaff

Abstract:	Remyelination is limited in the majority of multiple sclerosis (MS) lesions despite the presence of oligodendrocyte precursor cells (OPCs) in most lesions. This observation has led to the view that a failure of OPCs to fully differentiate underlies remyelination failure. OPC differentiation requires intricate transcriptional regulation, which may be disrupted in chronic MS lesions. The expression of few transcription factors have been

	differentially compared between remyelinating lesions and lesions refractory to remyelination. In particular, the oligodendrocyte transcription factor myelin regulatory factor (MYRF) is essential for myelination during development, but its role during remyelination and expression in MS lesions is unknown. To understand the role of MYRF during remyelination, we genetically fate mapped OPCs following lysolecithin-induced demyelination of the corpus callosum in mice and determined that MYRF is expressed in new oligodendrocytes. OPC-specific Myrf deletion did not alter recruitment or proliferation of these cells after demyelination, but decreased the density of new glutathione S-transferase π positive oligodendrocytes. Subsequent remyelination, in both the spinal cord and corpus callosum is highly impaired following Myrf deletion from OPCs. Individual OPC-derived oligodendrocytes, produced in response to demyelination, showed little capacity to express myelin proteins following Myrf deletion. Collectively, these data demonstrate a crucial role of MYRF in the transition of oligodendrocytes from a premyelinating to a myelinating phenotype during remyelination. In the human brain, we find that MYRF is expressed in NogoA and CNP-positive oligodendrocytes. In MS, there was both a lower density and proportion of oligodendrocyte lineage cells and NogoA+ oligodendrocytes expressing MYRF in chronically demyelinated lesions compared to remyelinated shadow plaques. The relative scarcity of oligodendrocyte lineage cells expressing MYRF in demyelinated MS lesions demonstrates, for the first time, that chronic lesions lack oligodendrocytes that express this necessary transcription factor for remyelination and supports the notion that a failure to fully differentiate underlies remyelination failure.

Title: Myelin Regulatory Factor Drives Remyelination in Multiple Sclerosis

Authors: Greg J. Duncan[1,2], Jason R. Plemel[6], Peggy Assinck[1,3], Sohrab B. Manesh[1,3], Fraser G.W. Muir[1,4,], Ryan Hirata[1], Matan Berson[1], Jie Liu[1], Michael Wegner[8], Ben Emery[9,10], G.R. Wayne Moore[1,4,7] and Wolfram Tetzlaff[1,2,5].

Affiliations: [1] International Collaboration on Repair Discoveries (ICORD), University of British Columbia (UBC), Vancouver, BC, Canada

[2] Department of Zoology

[3] Graduate Program in Neuroscience

[4] Pathology and Laboratory Medicine

[5] Department of Surgery

[6] Department of Clinical Neurosciences, Hotchkiss Brain Institute, University of Calgary, Calgary, Alberta Canada

[7] Vancouver Hospital and Health Sciences Centre

[8] Institut für Biochemie, Emil-Fischer-Zentrum, Friedrich-Alexander-Universität Erlangen-Nürnberg, Erlangen, Germany.

[9] School of Medicine, Jungers Center for Neurosciences Research, Oregon Health and Science University, U.S.A.

[10] Department of Anatomy and Neuroscience, University of Melbourne, Australia.

***Corresponding Author:**
Wolfram Tetzlaff, MD, PhD.
John and Penny Ryan British Columbia Leadership Chair in Spinal Cord Research
Professor, Departments of Zoology and Surgery
Director ICORD (International Collaboration on Repair Discoveries)
University of British Columbia
Blusson Spinal Cord Centre
818 West 10th Avenue
Vancouver, BC, V5Z 1M9
Phone: 604 675 8848
Fax: 604 675 8820
Email: tetzlaff@icord.org

Abstract

Remyelination is limited in the majority of multiple sclerosis (MS) lesions despite the presence of oligodendrocyte precursor cells (OPCs) in most lesions. This observation has led to the view that a failure of OPCs to fully differentiate underlies remyelination failure. OPC differentiation requires intricate transcriptional regulation, which may be disrupted in chronic MS lesions. The expression of few transcription factors have been differentially compared between remyelinating lesions and lesions refractory to remyelination. In particular, the oligodendrocyte transcription factor myelin regulatory factor (MYRF) is essential for myelination during development, but its role during remyelination and expression in MS lesions is unknown. To understand the role of MYRF during remyelination, we genetically fate mapped OPCs following lysolecithin-induced demyelination of the corpus callosum in mice and determined that MYRF is expressed in new oligodendrocytes. OPC-specific *Myrf* deletion did not alter recruitment or proliferation of these cells after demyelination, but decreased the density of new glutathione *S*-transferase π positive oligodendrocytes. Subsequent remyelination, in both the spinal cord and corpus callosum is highly impaired following *Myrf* deletion from OPCs. Individual OPC-derived oligodendrocytes, produced in response to demyelination, showed little capacity to express myelin proteins following *Myrf* deletion. Collectively, these data demonstrate a crucial role of MYRF in the transition of oligodendrocytes from a premyelinating to a myelinating phenotype during remyelination. In the human brain, we find that MYRF is expressed in NogoA and CNP-positive oligodendrocytes. In MS, there was both a lower density and proportion of oligodendrocyte lineage cells and NogoA+ oligodendrocytes expressing MYRF in chronically demyelinated lesions compared to remyelinated shadow plaques. The relative scarcity of oligodendrocyte lineage cells expressing MYRF in demyelinated MS lesions demonstrates, for the first time, that chronic lesions lack oligodendrocytes that express this necessary transcription factor for remyelination and supports the notion that a failure to fully differentiate underlies remyelination failure.

Keywords: remyelination, multiple sclerosis, MYRF, oligodendrocyte, Cre-loxP

Introduction

Multiple sclerosis (MS) is characterized by inflammatory CNS demyelination and is one of the most common causes of chronic motor disability in young adults [60]. Remyelination occurs in MS [49, 51], which is sufficient to restore conductance in experimental models [55] and potentially protect axons from degeneration [16, 26, 32, 44]. However, remyelination is often incomplete [46] with a lower percentage of remyelinating shadow plaques relative to demyelinated plaques at all ages [20] despite fewer acute inflammatory lesions with disease chronicity [19, 36]. While oligodendrocyte precursor cells (OPCs) and some premyelinating oligodendrocytes are found within chronically demyelinated MS lesions [7, 34, 61, 62], these lesions contain few oligodendrocytes capable of remyelination. This has led to the hypothesis that a failure of OPCs to fully differentiate causes remyelination failure in MS [14, 15, 34]. Oligodendrocyte differentiation requires intricate transcriptional regulation during development, but the role of many key transcription factors remain untested during remyelination [12]. We hypothesized that remyelination failure could result if the chronic lesion environment inhibits the expression of essential transcription factor(s) needed for oligodendrocyte differentiation or myelin gene expression.

Myelin regulatory factor (MYRF) is a transcription factor expressed in oligodendrocytes [5, 6, 11] and is essential for developmental myelination [11]. MYRF can directly bind putative enhancer sequences of myelin genes, such as *Mbp* and *Plp*, to induce their expression [5] and together with the transcription factor Sox10, synergistically promote myelin gene expression [11, 25]. Genetic deletion of *Myrf* during development results in a near complete failure to differentiate into late-stage myelinating oligodendrocytes yet does not overtly affect the specification of OPCs [11]. Therefore, *Myrf* deletion during development mirrors what is observed in chronically demyelinated MS lesions; OPCs are maintained within the CNS but cannot fully differentiate. At this time, no study has investigated the role of MYRF during remyelination nor its expression in MS lesions.

Here, we examined the function of MYRF during remyelination. By genetically fate mapping OPCs following lysolecithin (LPC) demyelination in the corpus callosum of mice, we found that MYRF was expressed in new oligodendrocytes. When *Myrf* was deleted in OPCs, their recruitment and proliferation within the lesion were not affected, but their capacity to differentiate into new oligodendrocytes was greatly diminished. OPC differentiation stalled at the premyelinating stage with recombined cells unable to express myelin proteins, ultimately inhibiting remyelination in both the corpus callosum and in the spinal cord. In human white matter, MYRF was expressed in Sox10+ oligodendrocyte lineage cells, which often co-labelled with the mature

oligodendrocyte marker NogoA. In the centres of chronic active MS lesions, there was a reduction in the density of MYRF+Sox10+ cells relative to both shadow plaques and normal-appearing white matter (NAWM). Additionally, fewer Sox10+ oligodendrocyte lineage cells, and Sox10+NogoA+ oligodendrocytes expressed MYRF in the lesion centres relative to shadow plaques, indicating these cells lacked expression of a necessary transcription factor for differentiation and myelination. Collectively, these data demonstrate that *Myrf* is essential for remyelination in the rodent CNS and its failure to be expressed in oligodendrocytes in chronic MS lesions is associated with remyelination failure.

Materials and Methods

Transgenic Mice and Experimental Design

Myrf$^{fl/fl}$ mice [11], which have LoxP inserted around exon 8 of *Myrf*, were crossed with PDGFRα-CreERT2 mice [52]. The Cre-mediated recombination of *Myrf* in the Myrf$^{fl/fl}$ mice was predicted to result in the production of a truncated protein that lacks the DNA-binding domain found in exon 8 and the C-terminus of the protein due to a frame shift, ultimately making the protein non-functional [11, 40]. Myrf$^{fl/fl}$ PDGFRα-CreERT2 (P-Myrf$^{fl/fl}$) mice were used to induce selective recombination and *Myrf* deletion in a portion of platelet-derived growth factor receptor α (PDGFRα)+ cells and Myrf$^{fl/wt}$ PDGFRα-CreERT2 (P-Myrf$^{fl/wt}$) littermates were used as controls. Myrf$^{fl/wt}$ mice demonstrate no phenotype following recombination compared to mice wildtype for *Myrf* [11, 40]. For genetic fate mapping experiments, Myrf$^{fl/fl}$ PDGFRα-CreERT2 lines were subsequently crossed with Rosa26R-eYFP (YFP) Cre-inducible reporter mice [56] or ROSA26-mGFP (mT/mG) [42] to induce, via Cre-mediated recombination, cytoplasmic or membrane-tethered fluorescence, respectively. Both Cre and inducible reporter genes were heterozygous in all experiments. All animals were genotyped prior to experiments via standard protocols. Myrf$^{fl/fl}$ mice were also crossed with PLP-CreERT2 and Rosa26-YFP mice to produce Myrf$^{fl/wt}$ and Myrf$^{fl/fl}$ PLP CreERT2 Rosa26-YFP mice to induce recombination in oligodendrocytes following tamoxifen injection.

Tamoxifen administration

Tamoxifen (T5648, Sigma) was dissolved in corn oil (C8267, Sigma) at 20mg/ml. P-Myrf^{fl} mice received intraperitoneal injections (100mg/kg) once daily for five days starting two days prior to lysolecithin demyelination. For Myrf$^{fl/wt}$ PLP CreERT Rosa26 YFP and Myrf$^{fl/fl}$ PLP CreERT Rosa26 YFP mice, 4-hydroxytamoxifen (H7904, Sigma) was dissolved in corn oil at 10mg/mL and 1mg was administered by intraperitoneal injection once per day

for five consecutive days. Tamoxifen improves the speed of remyelination at relatively low doses (0.5-2.0 mg/kg)[22] and results in cellular stress at high doses (75mg/kg) indicated by the upregulation of the Atf3 transcription factor [9]. To control for tamoxifen-mediated effects, all mice were treated with the same tamoxifen regiment except for a group of mice for qPCR and another for lesion size analysis at 3 days post lesion (DPL) which were injected with corn oil alone. We found that tamoxifen had no effect on lesion size at 3 DPL (tamoxifen treated 0.473 ± 0.099 mm^2 versus non-tamoxifen treated $0.376 \pm .027$ mm^2, P=0.355 Student's T-Test) suggesting that tamoxifen does not alter the susceptibility to lysolecithin-mediated demyelination.

Real-time quantitative PCR

2mm^3 blocks of the anterior corpus callosum and cortex were collected from P-Myrf$^{fl/fl}$ and P-Myrf$^{fl/wt}$ mice 12 days after the last tamoxifen or oil injection and flash frozen. RNA was extracted and reversed transcribed as previously described [48]. Primers for recombined *Myrf* [31] were normalized relative to β-actin and CT values were determined by automatic baseline and auto-threshold. ΔΔCT method was used to compare relative gene expression between groups [38].

Lysolecithin demyelination

1% lysophosphatidylcholine (lysolecithin L1381, Sigma) was dissolved in sterile phosphate-buffered saline (PBS) by sonication. Mice were deeply anaesthetized using a 3% isoflurane-oxygen mixture (Baxter) and a small hole was drilled with a dentist drill to allow for the insertion of a glass capillary attached to a 5 µL Hamilton syringe into the brain tissue. A total of 2µL was injected at a rate of 50nL/min by a pump (Precision Scientific Instruments) into the corpus callosum at the coordinates 1.4mm anterior to bregma, 1mm lateral of bregma and 2.1mm deep from the cortical surface. The glass capillary was retained in place for at least five minutes post injection to reduce reflux along the needle track. Mice received buprenorphine twice daily to alleviate pain (0.03mg/kg) for the first two days post-surgery and 1mL Ringer's solution. The overlying skin was sutured. For lysolecithin demyelination of the cervical spinal cord, surgeries were conducted as above with the following differences. A laminectomy of the C4 vertebrae was performed with fine surgical rongeurs. Injections were placed at a 30 degree angle relative to vertical and just lateral to the midline in the dorsal column to a depth of 0.5mm ventral to the dorsal surface. A total of 0.5µL of lysolecithin was injected at a rate of 50nL/min. The overlying musculature and skin were sutured.

Tissue processing

For immunohistochemical analysis of tissue, mice were deeply anaesthetized and transcardially perfused with PBS followed by 4% paraformaldehyde (04042, Fisher Scientific). Spinal cords or brains were dissected and postfixed in paraformaldehyde for either eight hours or overnight for brains. Tissue was then cryoprotected in ascending sucrose solutions before being embedded in OCT, frozen, and stored at -80^{o} Celsius. Tissue was sectioned coronally at 20µm thickness using a cryostat (HM-525, Thermo Scientific) and sections were thaw-mounted onto slides (12-550-15, Fisher Scientific).

To prepare tissue for electron microscopy, mice were deeply anaesthetized then perfused with 0.01M PBS before receiving 1% glutaraldehyde (16221, Electron Microscopy Sciences) with 4% paraformaldehyde at 4^{o} C. The area of demyelination was immediately dissected into 1mm^3 cubes and postfixed in 2% glutaraldehyde. Tissue was washed three times in 0.1M cacodylate buffer with 5.3mM $CaCl_2$ before being placed in 1% osmium tetroxide (19190, Electron Microscopy Sciences) with 1.5% potassium ferrocyanide (BDH) for 1.5 hours. Tissue was then dehydrated through ascending alcohol washes before embedding in Spurr resin.

Immunohistochemistry

Slides were thawed prior to staining and rehydrated with PBS. Sections were blocked using 10% donkey serum dissolved in PBS with 0.1% Triton. Primary antibodies (Supplementary Table 1) were applied overnight at room temperature in a humid chamber, washed, then appropriate donkey Dylight or Alexa Fluor secondary antibodies (Jackson ImmunoResearch Laboratories, Inc) were applied for two hours. Slides were subsequently washed and coverslipped using Fluoromount-G (0100-01, Southern Biotech). Prior to myelin stains, delipidation was performed using ascending and descending ethanol washes followed by PBS washes before the blocking step.

Cell counts and quantifications on mouse tissue

Imaging on mice was performed on a Zeiss Axio-Observer M1 inverted spinning disc confocal microscope using Zen 2011 or Zen 2 software. Tiled confocal merged images of the entire demyelinated zone in the corpus callosum were captured with a 40x oil immersion objective (numerical aperture 1.3) using a distance of 1µm between the individual optical sections. For cell counts, the lesion was defined by either the absence or obvious damage of myelin based on myelin basic protein (MBP) or 2',3'-cyclic-nucleotide 3'-phosphodiesterase (CNP) stains. The lesion area was defined by the presence of the astrocyte scar (increased GFAP+ density) for the analysis of the contribution of recombined cells to remyelination and analyses of the number of nodes of Ranvier. Five to seven sections were analyzed per animal beginning with the lesion epicenter. For analyses of the oligodendrocyte

density in the uninjured CNS, the corpus callosum contralateral to the lysolecithin injection were examined for PDGFRα+ and glutathione s-tranferases pi isoform (GSTπ)+ cells in the area dorsal of the ventricle.

To quantify node of Ranvier density systematic random sampling was conducted in the lesion and nodes of Ranvier were counted in 50µm x 50µm areas. Mature nodes of Ranvier were defined as punctate clusters of Ankyrin-G (AnkG) flanked by two punctate Caspr-positive paranodes [41]. Typically, over 1000 nodes were counted over 5-6 sections per animal. The density of SMI312+ axons were thresholded on ImageJ (NIH) and quantified as a percentage of lesion area. The volume of demyelinated tissue in P-Myrf$^{fl/fl}$ YFP and P-Myrf$^{fl/wt}$ YFP was examined by manually outlining the area of the intact corpus callosum that was MBP-negative.

To determine the area of demyelination that had been remyelinated by recombined cells in Myrf$^{fl/fl}$ PDGFRαCreERT2 mT/mG and Myrf$^{fl/wt}$ PDGFRαCreERT2 mT/mG mice, the lesion was imaged for GFP, MBP and GFAP. The ImageJ plugin 'RG2B Colocalization' was used to determine the area of GFP and MBP colocalization within the manually defined GFAP+ lesion.

Electron microscopy

Resin blocks with lysolecithin lesions were sampled every 250µm to determine the lesion epicenter. At the epicenter, 1µm semithin sections were cut on an ultramicrotome (Ultracut E, Reichert-Jung) and stained briefly in a 1% toluidine blue and 2% borax solution then coverslipped with Permount (SP15, Fisher Scientific). Rank analysis was performed [30] by two blinded raters on images of semithin sections of the whole dorsal column taken with a 63x oil immersion objective (numerical aperture 1.3) on a Zeiss, Axio Imager.M2 microscope. Each section was scored independently for the presence of thinly myelinated axons. When discrepancies in the ranking occurred, the average score was taken. For electron microscopy, ultrathin (90nm) sections of the lesion epicenter were collected and stained with Reynold's lead citrate and uranyl acetate to enhance contrast then imaged at 10000-12500x primary magnification on a Zeiss EM910.

Human tissue analysis

Human brain tissue was used with the approval of the UBC Clinical Research Ethics Board of the University of British Columbia (H01-70430). Patient information as well as the number of lesions analyzed for non-MS controls and MS patients is displayed in Supplementary Table 2. Sections (5µm) from formalin-fixed paraffin-embedded tissue were obtained on microtome (1512, Leitz) and all lesions were stained on adjacent slides with luxol fast blue (LFB), and immunohistochemically for class II human leukocyte antigen (HLA II), MBP and CNP for

lesion classification according to histological criteria [4, 59]. Only lesions within the subcortical or periventricular white matter were examined. NAWM was examined at least 1.0 cm distant from a lesion in an area lacking inflammation. For immunohistochemical staining, slides were first deparaffinized then antigen retrieval was performed by heating slides in pH 6.0 10mM sodium citrate buffer for ten minutes. Blocking was performed in 10% normal donkey serum in PBS Tween. Primary antibodies were applied overnight in a humid chamber before washing and applying appropriate Alexa Fluor conjugated secondary antibodies (Jackson ImmunoResearch Laboratories) at 1:200 for two hours. Slides were washed with PBS then stained with 0.30% (0.15% in slides with NogoA) Sudan black in 70% ethanol (4197-25-5, Sigma) for three minutes before being washed again in PBS and coverslipped with Fluoromount-G. An adjacent control slide for each lesion was stained simultaneously with secondary antibodies, Hoechst (1:10000) and Sudan black but lacked primary antibodies for comparison of background fluorescence. Cells were considered positive only if their fluorescence was substantially higher than background fluorescence as assessed on control slides imaged with the same exposure settings. Systematic random sampling was used within the lesion area manually defined on the Zen 2 software by Sudan black staining and cross-referenced with adjacent slides with HLA II and LFB staining. At least twenty 100µm x 100µm areas were examined in all lesions. Chronic lesions had 60 100µm x 100µm areas counted to increase the likely of detecting oligodendrocyte lineage cells.

Statistical Analyses

Statistical analyses were conducted on Statistical Package for Social Sciences software (IBM) and Graphpad (Prism) version 6.0. Parametric statistics were used assuming data met requirements for normality, tested by the Shapiro-Wilk test. For comparisons between two normally distributed groups, Student's t-test was used with or without the Welch correction depending on whether assumptions of the homogeneity of variance were met, analyzed by with Levene's test. The Mann-Whitney U-test was used to compare P-Myrf$^{fl/fl}$ to controls when the data was not normally distributed or was ordinal. A one-way ANOVA followed by Tukey's or Tamhane's *post hoc* test depending on whether there was equal homogeneity of variance between groups was used to compare three or more groups at one time point. For comparisons of cell counts between groups at different time points post-lysolecithin injection, a two-way ANOVA was run followed by Tukey's *post hoc* test. A unit was considered an individual animal or MS lesion. Individuals performing surgeries, cell counts and imaging were blinded to mouse genotype by a third party. For all tests, statistical significance was obtained if $P<0.05$ and all statistical tests were two-tailed. Data

are presented as the mean ± standard error of the mean. On graphs ns = not statistically significant, * = P≤0.05, ** = P≤0.01, ***P≤0.001 unless otherwise specified.

Results

MYRF is expressed in new oligodendrocytes during remyelination

The role of many oligodendrocyte transcription factors remains unstudied during remyelination, including MYRF. To investigate if MYRF is expressed in new oligodendrocytes during remyelination, we fate mapped OPCs using a tamoxifen-inducible Cre reporter line (Rosa26-eYFP) [56] in conjunction with an OPC inducible Cre-recombinase (PDGFRα-CreERT2) [52]. Mice were heterozygous for the *Myrf* floxed allele ($Myrf^{fl/wt}$). *Myrf* is haplosufficient and its function in oligodendrocytes is unchanged versus mice with two copies of the gene [11]. To induce reproducible demyelination, mice received an injection of lysolecithin into the genu of the corpus callosum (Fig. 1a). Remyelination following lysolecithin demyelination involves a stereotypic evolution [13]. OPCs proliferate and are recruited in the first 5 DPL, which is followed by prominent oligodendrocyte differentiation between 5-10 DPL and remyelination by ~14 DPL (Fig. 1a). Lysolecithin was very toxic to oligodendrocyte lineage cells and the majority of MYRF+ cells were lost at 3 DPL (Fig. 1b). However, by 7 and 14 DPL, MYRF+ cells increased in density relative to 3 DPL (Fig. 1c). Recombined yellow fluorescent protein positive (YFP+) cells rarely expressed MYRF at 3 DPL (10.28 ± 4.16%) but by 7 DPL 37.5% ± 4.00% of recombined cells expressed MYRF. To identify the cells expressing MYRF during remyelination, we assessed co-immunoreactivity of YFP with CC1 for oligodendrocytes (Fig. 1e) and PDGFRα for OPCs (Fig. 1f). While MYRF was not found expressed in OPCs (Fig. 1f), new oligodendrocytes (YFP+CC1+) were frequently observed to express nuclear MYRF staining at 7 DPL in P-$Myrf^{fl/wt}$ YFP mice (Fig. 1e). Collectively, MYRF+ cells were lost after lysolecithin-induced demyelination, and OPCs differentiate into new oligodendrocytes that express MYRF during remyelination.

Inducible deletion of Myrf from OPCs is sufficient to reduce MYRF expression within new oligodendrocytes

To uncover MYRF's function during remyelination, $Myrf^{fl/fl}$ PDGFRα CreERT2 Rosa26-eYFP mice (P-$Myrf^{fl/fl}$ YFP) were produced to delete *Myrf* and visualize OPCs and their progeny when tamoxifen had been administered. New oligodendrocytes (YFP+CC1+) in P-$Myrf^{fl/fl}$ YFP mice were less likely to express MYRF (Fig. 1e, g). Total MYRF density in P-$Myrf^{fl/fl}$ YFP mice declined by 32% at 7 DPL and 45% at 14 DPL relative to

controls (Supplementary Fig. 1S e). The MYRF antibody used here, raised against the N-terminus, should be capable of detecting the predicted truncated, non-functional protein product of the recombined allele. Nevertheless, the protein produced appears to be unstable and is only weakly detected in most recombined oligodendrocytes ([31] and Supplementary Fig. S1, 2, Fig. 1e, g). To explicitly determine if the inducible knockout effectively recombined *Myrf*, we examined the relative expression using a PCR primer sequence specific to recombined *myrf* mRNA lacking exon 8 [31]. P-Myrf$^{fl/fl}$ mice had increased levels of recombined *myrf* in the brain compared to P-Myrf$^{fl/fl}$ mice without tamoxifen (Fig. 1h). Taken together, conditional deletion of *Myrf* in OPCs was effective at reducing MYRF expression within new oligodendrocytes during remyelination.

MYRF is not required for recruitment or proliferation of OPCs but is crucial for their complete maturation into new oligodendrocytes following demyelination.

OPC recruitment is crucial for timely remyelination [47], and OPC proliferation is required for sustained oligodendrogenesis [53]. To determine directly if OPC recruitment or proliferation was altered by *Myrf* deletion, sections from P-Myrf$^{fl/fl}$ YFP and P-Myrf$^{fl/wt}$ YFP mice were examined for PDGFRα and the cell proliferation marker Ki67 to label cells in active stages of the cell cycle [54]. Both the non-recombined PDGFRα+ OPCs and recombined subpopulation expressed Ki67 after lysolecithin demyelination (Fig. 2a, d, e). *Myrf* deletion from OPCs did not alter the density of OPCs (Fig. 2b), the density of proliferating OPCs (Fig. 2c), the overall percentage of proliferating OPCs (Fig. 2f) or proliferation within recombined OPCs (Fig. 2g). Therefore, MYRF is not required for OPC proliferation or recruitment to demyelinated lesions.

To determine how *Myrf* deletion from OPCs affects their subsequent differentiation and maturation during remyelination, we first examined whether recombined cells continued to express the OPC marker PDGFRα or have differentiated and express CC1 (Fig. 3a). At 3, 7 and 14 DPL the percentage of recombined cells that expressed CC1 or PDGFRα did not differ between P-Myrf$^{fl/fl}$ YFP and P-Myrf$^{fl/wt}$ mice (Fig. 3b, c). Given that CC1 was expressed early after lysolecithin-induced demyelination before the onset of significant remyelination (Supplementary Fig. S3), we reasoned that MYRF might be dispensable for early differentiation of oligodendrocytes into a premyelinating phenotype, but crucial for the expression of later markers of oligodendrocyte differentiation. At 7 DPL, a time point in which CC1+ cells were abundant within the lesion, staining with the oligodendrocyte marker GSTπ, indicates that GSTπ+ cells are largely absent from the lesion (Supplementary Fig. S3). However, by 14 DPL,

GSTπ+ cells were found throughout the lesion (Fig. 3d), suggesting GSTπ labels a later stage of oligodendrocyte development relative to CC1. Recombined cells from P-Myrf$^{fl/fl}$ YFP and P-Myrf$^{fl/wt}$ YFP mice were examined for GSTπ and CNP expression at 7 and 14 DPL (Fig. 3d, e, f). In P-Myrf$^{fl/fl}$ YFP mice, a lower percentage of recombined cells expressed CNP (Fig 3g) and GSTπ (Fig. 3h) relative to controls at 14 DPL. There was also an overall decrease in the total density of GSTπ+ cells in P-Myrf$^{fl/fl}$ YFP mice, despite recombination in only a portion of OPCs (Fig. 3i). Thus during remyelination, markers expressed later in the differentiation of OPCs into oligodendrocytes, like GSTπ, were increasingly diminished relative to early differentiation markers like CC1 following *Myrf* deletion.

Decreased expression of GSTπ could not be accounted for by increased differentiation of OPCs into other cell types including astrocytes, as *Myrf* deletion did not increase the proportion of cells expressing GFAP during remyelination and over 95% of recombined cells have nuclear Olig2 suggesting they remain within the oligodendrocyte lineage (Supplementary Fig. S4). In sections from a complimentary cohort of P-Myrf$^{fl/fl}$ and P-Myrf$^{fl/wt}$ mice lacking the Rosa26-eYFP inducible reporter, sections were co-stained with Olig2 in combination with stage-specific markers of oligodendrocyte maturation to ensure that changes in OPC and oligodendrocyte densities could not be attributable to labelling of CC1 or PDGFRα in other cell types (Supplementary Fig. S5). Like in inducible reporter-positive mice, we found no change in OPC recruitment (Supplementary Fig. S5 b, e), or the onset of differentiation (Olig2+CC1+ cells) at 5 DPL but a decrease in Olig2+ density and Olig2+CC1+ oligodendrocytes at 10 DPL (Supplementary Fig. S5 d, f). Collectively, these data indicate MYRF is not required for OPC proliferation, recruitment or initial differentiation but is required for the expression of late-stage oligodendrocyte markers during remyelination.

Myrf deletion from OPCs leaves new oligodendrocytes prone to apoptosis

Increased apoptosis occurs in the optic nerve of Myrf$^{fl/fl}$ Olig2 Cre mice during development [11] and in the adult spinal cord following inducible *Myrf* deletion from mature oligodendrocytes [31]. To determine whether the absence of *Myrf* increases apoptosis of oligodendrocytes following demyelination, we examined cleaved caspase-3 (CCasp3) expression in P-Myrf$^{fl/fl}$ and P-Myrf$^{fl/wt}$ mice (Fig. 4a, b). We found no overall difference in CCasp3+ cell density between P-Myrf$^{fl/fl}$ and P-Myrf$^{fl/wt}$ mice at either 5 or 10 DPL (Fig. 4c), likely because the majority of the apoptotic cells co-labelled with the pan-leukocyte marker CD45 (Fig. 4b) or the microglial/macrophage marker Iba1

(Fig. 4d, e). However, occasional CC1+CCasp3+ cells were observed (Fig. 4f). The density of CC1+ oligodendrocytes undergoing apoptosis was increased by approximately 4-fold at 10 DPL in P-Myrf$^{fl/fl}$ mice (Fig. 4g). Similarly, the percentage of oligodendrocytes that were CCasp3+ was higher at 10 DPL (Fig. 4h). However, oligodendrocytes comprised the minority of apoptotic cells, even in P-Myrf$^{fl/fl}$ mice (Fig. 4i). The truncated protein predicted to be produced in P-Myrf$^{fl/fl}$ mice is unlikely to be directly apoptotic to oligodendrocytes as recombined oligodendrocytes persist in Myrf$^{fl/fl}$ PLP-CreERT2 mice for weeks following *Myrf* deletion (Supplementary Fig. 2S and [31]). During remyelination, oligodendrocytes are overproduced [21], similar to developmental myelination, and compete for axonal-derived cues necessary for survival [2, 3]. New oligodendrocytes lacking *Myrf* undergo apoptosis, presumably due to impaired stabilization, ensheathment or access to axonal-derived cues. Collectively, these data suggest impairing the later stages of oligodendrocyte differentiation by deleting *Myrf* leaves oligodendrocytes vulnerable to apoptosis during remyelination.

Myrf deletion from OPCs does not induce overt demyelination, astrogliosis, or inflammation in the first two weeks following recombination

There is a continual production of new oligodendrocytes in adulthood [29, 52]. *Myrf* deletion from OPCs inhibits the formation of new oligodendrocytes during motor learning [40, 63] and could plausibly induce demyelination by impairing the differentiation of new oligodendrocytes in the healthy CNS. To determine if *Myrf* deletion resulted in demyelination in the healthy CNS during the first two weeks, we assessed myelin status by staining the uninjured side of the corpus callosum contralateral to lysolecithin injection with the myelin protein MBP (Fig. 5a, a', e, e'). We observed no overt signs of demyelination of the uninjured corpus callosum 14 DPL in P-Myrf$^{fl/fl}$ YFP mice and GSTπ+ oligodendrocytes were readily observed (Fig. 5b, b', f, f'). Electron microscopy revealed compact myelination in both control and P-Myrf$^{fl/fl}$ YFP mice at 14 DPL in the uninjured corpus callosum and spinal cord (Fig. 6c). Astrogliosis (Fig. 5c, c', g, g') was not observed nor clustering of microglia or obvious changes in their morphology (Fig 5d, d', h, h'), in either P-Myrf$^{fl/fl}$ YFP or P-Myrf$^{fl/wt}$ YFP mice. The total density of GSTπ+ oligodendrocytes (Fig. 5k) and PDGFRα+ OPCs (Fig. 5l) did not differ at 14 DPL in the contralateral non-injected corpus callosum. However, when the recombined subpopulations were examined for GSTπ (Fig. 5i) or PDGFRα (Fig. 5j), a higher percentage were found to express PDGFRα in P-Myrf$^{fl/fl}$ YFP mice compared to P-Myrf$^{fl/wt}$ YFP mice (Fig. 5m). Recombined cells in P-Myrf$^{fl/fl}$ YFP mice rarely expressed GSTπ (2.41% ± 0.83%),

whereas in P-Myrf$^{fl/wt}$ YFP mice, 15.10% ± 3.83% expressed GSTπ. Thus, *Myrf* deletion from OPCs prevents the formation of new late-stage oligodendrocytes in the healthy brain as well as the demyelinated brain, but does not result in overt demyelination, astrogliosis or inflammation during the first two weeks after deletion.

MYRF is essential for remyelination

Myrf deletion lowered the density of new GSTπ+ oligodendrocytes in response to demyelination, and as a consequence should reduce the efficiency of remyelination. We examined remyelination in semithin sections of the dorsal column 14 DPL in P-Myrf$^{fl/fl}$ and P-Myrf$^{fl/wt}$ mice (Fig. 6a). The spinal cord has larger calibre axons relative to the corpus callosum allowing remyelinated axons to be easily distinguished based on their thinner myelin. This is in contrast to the corpus callosum, which has many smaller axons (< 1µm) that do not always demonstrate thinner myelin during remyelination [1]. In the spinal cords of control mice, numerous thinly myelinated axons, suggestive of remyelination, were found (Fig. 6b, c). In contrast, there was a scarcity of thinly myelinated axons in P-Myrf$^{fl/fl}$ mice (Fig. 6b, c) that was confirmed by blinded rank analysis (Fig. 6d). We also examined the presence of MBP staining in the corpus callosum to determine the extent of demyelination following lysolecithin injection in P-Myrf$^{fl/fl}$ YFP and P-Myrf$^{fl/wt}$ YFP mice. (Fig. 6e, f). The volume of demyelination (area lacking MBP staining) did not differ at 3 or 7 DPL, indicating *Myrf* deletion from OPCs did not leave the callosum more susceptible to myelin loss. However, by 14 DPL there was a larger demyelinated area in P-Myrf$^{fl/fl}$ YFP mice compared to controls (Fig. 6e) suggestive of impaired remyelination. Thus, in two cohorts of animals, in two different regions of the CNS, MYRF was crucial for effective remyelination.

Remyelination can restore conductance [55], likely in part through clustering of sodium channels [18]. Clustering of sodium channels at nodes of Ranvier does not typically occur in the absence of oligodendrocytes and myelination in the CNS [39]. To assess whether *Myrf* deletion from OPCs impaired the restoration of nodes of Ranvier in lysolecithin-demyelinated lesions in the corpus callosum, we stained tissue with AnkG—to identify the sodium channel scaffolding protein at the nodes—and Caspr to label paranodes. We counted nodes of Ranvier as those with punctate Caspr surrounding AnkG staining (Fig. 6i) [41]. *Myrf* deletion reduced the density of nodes of Ranvier within the lesion (Fig. 6g). Less axons within the lesion could also diminish node of Ranvier density, but no differences in the density of SMI312+ axons were observed (Fig 6h). Thus, these data suggest a reduction of node of Ranvier density is due to reduced oligodendrogenesis and not due to axon loss.

To examine axon-oligodendrocyte contact and remyelination directly in recombined cells, we crossed P-Myrf$^{fl/fl}$ and P-Myrf$^{fl/wt}$ mice with a reporter line (mT/mG) that expressed Cre-inducible membrane-anchored GFP (Fig. 7a) [42]. The membrane-anchored inducible GFP allows for the visualization of ensheathment and myelination of axons by new oligodendrocytes [29]. At 28 DPL in P-Myrf$^{fl/wt}$ mT/mG mice, OPCs were recruited to the lesion, differentiated, and extended processes that co-label with MBP (Fig. 7b, d, e). In contrast, recombined cells in P-Myrf$^{fl/fl}$ mT/mG mice increased in density near the lesion but rarely co-label with MBP (Fig. 7b, d, e). There was a large reduction in the capacity of recombined cells to produce myelin at 28 DPL (Fig 7c). While non-recombined cells produced myelin normally in P-Myrf$^{fl/fl}$ mT/mG mice, this was not sufficient to compensate for the recombined cells and resulted in incomplete remyelination even at 28 DPL (Fig. 7c). Taking advantage of the larger axon calibre in the spinal cord relative to the corpus callosum, we examined ensheathment and myelination of individual axons by new oligodendrocytes in the dorsal column. While new oligodendrocytes (CC1+GFP+) were found to wrap axons and produced MBP in control P-Myrf$^{fl/wt}$ mT/mG mice following demyelination (Fig. 7f, g) new oligodendrocytes in P-Myrf$^{fl/fl}$ mT/mG mice occasionally ensheathed axons but failed to express MBP (Fig. 7f, h). These data demonstrate that MYRF is required for the expression of myelin proteins in new oligodendrocytes. Notably, *Myrf* deletion from OPCs does not prevent the formation of myelinating Schwann cells (P0+) from recombined cells following demyelination in the spinal cord (Supplementary Fig. S6).

MYRF expression within oligodendrocytes is correlated with successful remyelination in MS

Remyelination often fails in MS [20, 46]. The expression of few transcription factors has been differentially compared in human tissue between remyelinated 'shadow plaques' and chronically demyelinated lesions. Given the crucial role of MYRF in rodent remyelination, we examined MYRF and the oligodendrocyte-lineage marker Sox10 [58, 64] in both the healthy white matter and in periventricular and subcortical white matter lesions (Fig. 8a, b). MYRF was expressed in Sox10+ cells (Fig. 8c). Faint MYRF immunoreactivity was observed along blood vessels or in myelin sheaths/debris. However, MYRF was not typically detected in Iba1+ microglia or GFAP+ astrocytes in NAWM (Supplementary Fig. S7). In NAWM, MYRF was expressed in cells with strong NogoA expression (Supplementary Fig. S8), CNP+ cells in remyelinated shadow plaques (Fig 8d), and in NogoA+ cells within the active rims and centres of chronic lesions (Fig. 8e). CNP and NogoA are established markers of differentiated

oligodendrocytes in human tissue [34, 35, 50], and our data demonstrate that MYRF is expressed in oligodendrocytes in the human CNS.

To assess whether MYRF expression is associated with remyelination in MS, we quantified the density of Sox10+MYRF+ cells within lesions and NAWM. The density of both Sox10+ oligodendrocyte lineage cells and Sox10+MYRF+ oligodendrocytes were reduced in the centre of chronic lesions relative to shadow plaques, chronic active lesion rims and NAWM, indicating a depletion of both oligodendrocyte lineage cells and MYRF-expressing oligodendrocytes within chronic lesions (Fig. 8f, g Supplementary Fig. S9). The percentage of Sox10+ cells expressing MYRF was also reduced in chronic lesion centres relative to shadow plaques and NAWM (Fig. 8h). We next examined NogoA, Sox10 and MYRF staining in chronic active lesions, NAWM and shadow plaques. Fewer Sox10+ cells expressed strong NogoA in chronic active lesion centres relative to shadow plaques (Supplementary Fig. S8 b), suggesting an accumulation of OPCs relative to oligodendrocytes. However, there was also a decreased percentage of Sox10+ strongly NogoA+ oligodendrocytes expressing MYRF within chronic active lesion centres relative to both chronic lesion rims, shadow plaques, and NAWM (Fig. 8i), indicating there was also a population of differentiated oligodendrocytes unable to express detectable MYRF specifically in lesion centres. Collectively, the increased density and capacity of oligodendrocytes to express MYRF in areas of remyelination demonstrates that MYRF is associated with successful remyelination in the MS lesions examined.

Discussion

Many transcription factors crucial for developmental myelination remain poorly characterized during remyelination, including MYRF. Using an inducible deletion of *Myrf* from OPCs concurrent with a focal demyelinating lesion, we demonstrated that MYRF is not expressed in OPCs in the healthy or demyelinated CNS, and their proliferation and recruitment to demyelinated lesions is not altered by *Myrf* deletion. However, genetic fate mapping revealed that in the absence of *Myrf*, OPCs initially differentiate but are unable to robustly express late-stage oligodendrocyte markers or myelin proteins. Thus, *Myrf* deletion from OPCs stalls their differentiation at the premyelinating stage during remyelination (Supplementary Fig. S10). In human white matter, Sox10+NogoA+ oligodendrocytes were found to be positive for MYRF protein expression. We encountered fewer Sox10+MYRF+ cells in chronically demyelinated lesions. Additionally, a lower proportion of oligodendrocyte lineage cells expressed MYRF in chronic lesion centres compared to shadow plaques or NAWM indicating a strong association

of MYRF expression with remyelination in MS. Collectively, our findings implicate MYRF in orchestrating myelin regeneration in both the rodent and human CNS.

Oligodendrocyte lineage cells in chronic MS lesions lack expression of the transcription network required for myelination

In chronic MS lesions, we find a deficiency of MYRF-expressing oligodendrocytes relative to shadow plaques and NAWM. MYRF together with Sox10 constitute an essential regulatory network that drives myelin gene expression [25]. The lack of MYRF expression in Sox10+ cells from chronic lesions could be a result of an accumulation of OPCs relative to oligodendrocytes, supporting the notion that remyelination failure results from impaired OPC differentiation [34, 61, 62]. Accordingly, we find a lower percentage of Sox10+ cells express strong NogoA within chronic lesions centres relative to NAWM, suggestive of a failure to initially differentiate. However, we also detect a population of Sox10+NogoA+ oligodendrocytes unable to express MYRF within chronic lesion centres. NogoA is not typically expressed in OPCs [35], suggesting that these cells have differentiated but fail to express MYRF and would, therefore, be unable to remyelinate. These data raise the possibility that even if OPCs are able to initially differentiate, the inhibitory environment of the chronic MS lesions examined may prevent MYRF expression, the later stages of differentiation, and subsequent remyelination. In mice, we demonstrated that MYRF is crucial for the survival of newly generated oligodendrocytes, so an inability to express MYRF in oligodendrocytes may leave them vulnerable to apoptosis. Over time, this could contribute to the severe depletion of oligodendrocytes observed in most chronic MS lesions.

Nonetheless, in all chronic active lesions examined occasional Sox10+MYRF+ cells are found, suggesting there is a population of oligodendrocytes expressing the necessary transcription factors for remyelination, yet these cells are apparently unable to successfully remyelinate these lesions. This finding is in accordance with previous research which indicates a population of myelin proteolipid protein expressing (PLP+) oligodendrocytes fail to radially wrap axons and successfully remyelinate in the majority of chronically demyelinated lesions [7]. Collectively, these data imply remyelination failure in chronic lesions may be *multifactorial*. OPC differentiation failure, which we define as the inability transition from a proliferative OPC to post-mitotic oligodendrocyte, along with myelination failure, or the inability to wrap axons and deposit myelin, may both contribute to remyelination failure. Conduction deficits in axons of chronically demyelinated lesions may inhibit effective differentiation [21]

and/or stabilization of oligodendrocyte wraps and subsequent myelination [24]. Additionally, inhibitory substrates on axons such as polysialylated-neural cell adhesion molecule[8], myelin debris [33, 48], extracellular molecules like fibronectin [57] and chondroitin sulfate proteoglycans (CSPGs) [30] may inhibit remyelination. Together these and other factors could leave oligodendrocyte lineage cells in chronic MS lesions unable to express MYRF and subsequently remyelinate axons.

Eliciting MYRF expression within oligodendrocyte lineage cells of chronic lesions may be a crucial step to promote remyelination in MS. A greater understanding of the signaling pathways that induce MYRF expression within premyelinating oligodendrocytes and the inhibitory influence of chronic MS lesions on these pathways will be of critical importance for designing new therapeutics to overcome remyelination failure. Deletion of extracellular signal–regulated kinases 1/2 (ERK1/2) in oligodendrocytes reduced the expression of *myrf* during development and in the healthy CNS [27]. Conversely, sustained activation of the ERK1/2 increases *myrf* expression and reinitiates myelination in quiescent oligodendrocytes in the uninjured and demyelinated CNS [28]. The antifungal agent miconazole, which results in the sustained phosphorylation of ERK1/2 in OPCs, has been shown to accelerate remyelination [43]. Targeting the phosphorylation of ERK1/2 with miconazole or other compounds may stimulate MYRF expression and possibly overcome the inhibitory milieu of the chronic lesion and enhance remyelination.

The Role of MYRF in Remyelination Broadly Recapitulates Developmental Myelination

During both developmental myelination and remyelination, OPCs proceed through the same stages of maturation from OPC to myelinating oligodendrocyte [12, 17]. This process requires the differential expression of transcription factors at distinct stages of maturation [10]. We find that during remyelination, MYRF was expressed with the onset of differentiation at the premyelinating stage after the downregulation of the OPC mitogen receptor PDGFRα, and nearly concurrent with the expression of CC1. Given that MYRF is not expressed in OPCs during remyelination, it is not surprising its deletion does not alter OPC recruitment or proliferation. Recombined cells lacking MYRF can initially differentiate but have reduced expression of the more mature markers GSTπ and CNP and ultimately fail to express the myelin protein MBP. Thus, during remyelination, MYRF has a unique combination of characteristics amongst oligodendrocyte transcription factors; it is only expressed after initial OPC differentiation, regulates the transition from premyelinating to myelinating oligodendrocyte, and is crucial for myelin gene expression.

Myrf deletion from OPCs will be a useful tool to examine the extent and mechanisms by which remyelination protects axons

Oligodendrocytes have been theorized to support axonal survival [44]. While many studies [23, 37, 45] provide strong support for an essential role of oligodendrocytes in the health of axons, little *causative* evidence exists that oligodendrocyte remyelination is sufficient to preserve axons during inflammatory demyelination. This is, in large part, due to the difficulty of decoupling oligodendrogenesis and remyelination from inflammation and other degenerative processes during demyelination. Several therapies targeting remyelination in MS are entering clinical trials, and it will be crucial to determine the relative effectiveness and timeframe by which remyelination may prevent axon loss following inflammatory demyelination.

P-Myrf$^{fl/fl}$ mice may be an excellent model to assess the sufficiency and mechanisms by remyelination protects axons following demyelination. Lesions in P-Myrf$^{fl/fl}$ mice resemble those of chronic MS lesions, in that these lesions contain OPCs and premyelinating oligodendrocytes, but few oligodendrocytes capable of remyelinating axons. Inducible *Myrf* deletion from OPCs does not result in overt signs of demyelination, reactive astrogliosis, or inflammatory lesions during the timeframe of our study, which could confound an interpretation of the role of remyelination on axonal health. MYRF is also not expressed in OPCs nor alters their proliferation or recruitment to areas of demyelination. Given that non-recombined cells can remyelinate normally in P-Myrf$^{fl/fl}$ mice, a higher recombination efficiency of *Myrf* from OPCs would have been ideal. A second PDGFRα CreERT2 line developed independently to the one used in this study has a higher recombination efficiency throughout the CNS [29]. This line combined with autoimmune or cuprizone demyelination should result in long-term demyelination and thus be a suitable tool to assess the efficacy, rate, and mechanisms by which new oligodendrocytes and remyelination may protect axons from degeneration and enhance recovery following remyelination failure.

Collectively, our work demonstrates that MYRF is essential for successful remyelination by acting as a master regulator crucial for the transition of oligodendrocytes from a premyelinating to myelinating phenotype. We establish, for the first time, that chronic MS lesions lack oligodendrocytes that express this necessary transcription factor for remyelination. Eliciting MYRF expression in oligodendrocyte lineage cells may be essential for overcoming remyelination failure in MS.

Acknowledgements

The PDGFRα CreERT line used in this study was a generous gift of Dr. William Richardson. The NogoA antibody used in the study was a kindly provided by Dr. Martin Schwab. We also thank Dr. Terry Joe Sprinkle for the antibody to CNP. Yasaman Chaeichi, Phillip Chau and Arash Samiei are acknowledged for their technical assistance with cryostat sectioning and confocal microscopy. The authors would like to thank Susan Shin for her help with electron microscopy sectioning and imaging. Michael J. Lee is acknowledged for his assistance with transgenic breeding and genotyping. Vladimira Pavlova and Zahra Samadi-Bahrami for histological sectioning and immunofluorescence staining of human tissue. We also thank Dr. Brett Hilton for his critical reading and editing of this manuscript.

Compliance with ethical standards

All animal experiments were approved by the University of British Columbia Animal Care Committee, in accordance with the guidelines of the Canadian Council on Animal Care.

Conflict of interest

The authors declare that they have no competing interests.

Funding

This study was supported by operating grants from the Multiple Sclerosis Society of Canada (EGID 1763 and 2810) and the Canadian Institutes of Health Research (MOP-130475). G.J.D. is supported by a Multiple Sclerosis Society of Canada Doctoral Scholarship. J.R.P is supported Donna Joan Oxford Postdoctoral Fellowship Award from the Multiple Sclerosis Society of Canada and postdoctoral fellowship awards from CIHR, T. Chen Fong and Alberta Initiatives Health Solutions. P.A. received a Frederick Banting and Charles Best Canadian Graduate Scholarship-Doctoral Award. S.B.M. and F.G.W.M by a Multiple Sclerosis Society of Canada Masters' studentship. M.W. holds a Deutsche Forschungsgemeinschaft grant (We1326/11). B.E. is supported by a project grant from the National Multiple Sclerosis Society (RG5106A1/1) and a Warren Distinguished Scholar in Neuroscience Research chair. G.R.W.M. is supported by an operating grant from the Multiple Sclerosis Society of Canada (EGID 2295). W.T. holds the John and Penny Ryan British Columbia Leadership Chair in Spinal Cord Research.

Figure Legends

Fig. 1 MYRF is expressed in new oligodendrocytes following focal demyelination. **a** Schematic of the transgenic mice used, lysolecithin injection location and experimental timeline. **b** Micrographs of MYRF and YFP expression in demyelinating lesions at 3, 7 and 14 DPL in P-Myrf$^{fl/wt}$ YFP mice. Dashed line demarcates the approximate lesion boundary. **c** Quantification of MYRF+ cell density demonstrates increased density in P-Myrf$^{fl/wt}$ YFP mice between 3 and 7 DPL *(P=0.013*) and 3 and 14 DPL (P<0.001). **d** Quantification indicating an increase in the percentage of recombined cells (YFP+) which are also MYRF+ by 7 DPL (P=0.001) and 14 DPL (P<0.001) relative to 3 DPL. **e** Micrographs demonstrating that some recombined cells have differentiated and express the mature oligodendrocyte marker CC1, which often co-label with MYRF (arrowheads) in P-Myrf$^{fl/wt}$ YFP mice 7 DPL. In P-Myrf$^{fl/fl}$ YFP mice, many recombined cells have either faint or undetectable expression of MYRF in newly differentiated oligodendrocytes (arrows). **f** Micrograph indicating MYRF is not expressed in PDGFRα+ cells in lesions or adjacent to lesion boundaries (dashed line). **g** Quantification demonstrating the percentage of recombined oligodendrocytes (CC1+YFP+) that express MYRF is reduced at 7 DPL (*P<0.001),* and 14 DPL (*P=0.016*) in P-Myrf$^{fl/fl}$ YFP relative to P-Myrf$^{fl/wt}$ YFP mice. **h** Quantification using primers specific for recombined *myrf* (lacking exon 8) shows there is an increase in expression within the brain of P-Myrf$^{fl/fl}$ mice treated with tamoxifen (*P=0.036)* compared to P-Myrf$^{fl/fl}$ mice that did not receive tamoxifen. Two-way ANOVA followed by Tukey's *post hoc* test in **c**, **g** and Tamhane's *post hoc* test in **d.** *n*=4-6 mice per group per timepoint in **c**, **d** and **g**. Kruskal-Wallis test followed by Dunn's test, *n*=3-4 per group in **h**. Scale bars are 50 µm in **b** and 20µm in **e** and **f**

Fig. 2 MYRF is not required for OPC recruitment or proliferation in demyelinated lesions. **a** Representative photomicrographs of lesion epicentre stained for CNP and Ki67 or YFP and PDGFRα in P-Myrf$^{fl/wt}$ YFP and P-Myrf$^{fl/fl}$ YFP mice 3 DPL. Dashed line demarcates approximate lesion boundary. **b** Quantification of PDGFRα+ cell density indicates there is no difference between P-Myrf$^{fl/fl}$ YFP and P-Myrf$^{fl/wt}$ YFP mice at any time point. **c** Quantification demonstrating Ki67+PDGFRα+ cell density does not differ between P-Myrf$^{fl/wt}$ YFP and P-Myrf$^{fl/fl}$ YFP mice at 3, 7 or 14 DPL, but declines between 3 DPL and 7 DPL in both groups (*P-Myrf$^{fl/wt}$ YFP P<0.001, P-Myrf$^{fl/fl}$ YFP P=0.002*). **d** Single optical confocal section demonstrating co-labelling between YFP, PDGFRα, and Ki67 (arrowheads) in P-Myrf$^{fl/wt}$ YFP and **e** P-Myrf$^{fl/fl}$ YFP mice. Arrows indicate YFP+PDGFRα+Ki67- cells. **f** Quantification indicating the percentage of PDGFRα+ cells which express Ki67 does not differ between P-Myrf$^{fl/fl}$

and P-Myrf$^{fl/wt}$ mice at any time point, but declines between 3 and 7 DPL in both P-Myrf$^{fl/wt}$ YFP (*P<0.001*) and P-Myrf$^{fl/fl}$ YFP (*P<0.001*) mice. **g** Quantification demonstrating the percentage of recombined OPCs (YFP+PDGFRα+) that are Ki67+ does not differ between P-Myrf$^{fl/wt}$ YFP and P-Myrf$^{fl/fl}$ YFP mice at any time point examined but declines between 3 and 7 DPL in both P-Myrf$^{fl/wt}$ YFP (*P<0.001*) and P-Myrf$^{fl/fl}$ YFP (*P<0.001*) mice. Scale bars are 50µm in **a** and 10µm in **d**, and **e**. Two-way ANOVA followed by Tukey's *post hoc* test for **b**, **c**, **f**, **g**. *n*=4-6 mice per group per timepoint.

Fig. 3 *Myrf* deletion does not alter the transition from an OPC to premyelinating oligodendrocyte, but inhibits the later stages of oligodendrocyte differentiation during remyelination. **a** Photomicrographs of a single optical confocal section of the lesion at 7 DPL. Recombined cells within lesions express either CC1 (arrowheads) or PDGFRα (arrows), in both P-Myrf$^{fl/wt}$ YFP and P-Myrf$^{fl/fl}$ YFP mice. **b** Quantification demonstrating the percentage of recombined cells that are CC1+does not differ at any time point examined between P-Myrf$^{fl/wt}$ YFP and P-Myrf$^{fl/fl}$ YFP mice but increases in both groups between 3 and 14 DPL (*P-Myrf$^{fl/wt}$ YFP P<0.001, P-Myrf$^{fl/fl}$ YFP P<0.001*). **c** Quantification of demonstrating the percentage of recombined cells that are PDGFRα+ does not differ between P-Myrf$^{fl/wt}$ YFP and P-Myrf$^{fl/fl}$ YFP mice at any time point examined; but the percentage of cells declines in both groups between 3 and 14 DPL (*P-Myrf$^{fl/wt}$ YFP P=0.003, P-Myrf$^{fl/fl}$ YFP P=0.002*). **d** Representative photomicrograph of lesion epicentre 14 DPL in both P-Myrf$^{fl/wt}$ YFP and P-Myrf$^{fl/fl}$ YFP mice stained for YFP, GSTπ and CNP. Dashed lines demarcate lesion boundaries. **e** Single optical section demonstrating considerable co-labelling between YFP, GSTπ (arrowheads) and CNP in P-Myrf$^{fl/wt}$ YFP mice 14 DPL. **f** Recombined cells in P-Myrf$^{fl/fl}$ YFP mice rarely express GSTπ. **g** Quantification demonstrating that the percentage of recombined cells that are CNP+ (*P=0.021*) and **h** GSTπ+ (*P<0.001*) declines in P-Myrf$^{fl/fl}$ YFP compared to P-Myrf$^{fl/wt}$ YFP mice at 14 DPL **i** Quantification indicating the total GSTπ+ cell density is reduced within the lesion at 14 DPL in P-Myrf$^{f/fl}$ YFP compared to P-Myrf$^{fl/wt}$ YFP mice (*P=0.043*). All statistical comparisons in **b**, **c**, **g**, **h**, **i** used a two-way ANOVA followed by Tukey's *post hoc* test, *n*=4-6 mice per group per timepoint. Scale bars are 20µm in **a**, **e** and **f** and 50µm in **d**

Fig. 4 Oligodendrocytes are more prone to apoptosis following *Myrf* deletion from OPCs during remyelination. **a** Representative photomicrographs of demyelinated lesion stained for MBP and CCasp3 at 5 and 10 DPL in both P-Myrf$^{fl/wt}$ and P-Myrf$^{fl/fl}$ mice. Dashed line demarcates approximate lesion boundary. **b** Micrograph of the lesion

epicentre stained with CD45 and CCasp3 in P-Myrf$^{fl/wt}$ and P-Myrf$^{fl/fl}$ mice at 10 DPL. The majority of CCasp3+ cells associate with CD45. **c** Quantification of total CCasp3+Hoechst+ (apoptotic) cell density. **d** Single optical confocal section demonstrating that CCasp3+ is expressed in CD45+ cells (arrowhead), and many cells also express the microglia/macrophage marker Iba1 in both P-Myrf$^{fl/wt}$ and **e** P-Myrf$^{fl/fl}$ mice. **f** Single optical confocal section at 10 DPL in P-Myrf$^{fl/fl}$ mice, with single channels of Hoechst, CC1 and CCasp3. Arrowhead indicates CC1+Hoechst+CCasp3+ cell. **g** Quantification indicating CC1+CCasp3+ density is higher in P-Myrf$^{fl/fl}$ compared to P-Myrf$^{fl/wt}$ mice at 10 DPL (*P=0.039*). **h** Quantification demonstrating increased percentage of CC1+ cells are CCasp3+ in P-Myrf$^{fl/fl}$ compared to P-Myrf$^{fl/wt}$ mice at 10 DPL (*P=0.028*). **i** Quantification revealing an increase at 10 DPL in the percentage of apoptotic cells that express CC1 in P-Myrf$^{fl/fl}$ relative to P-Myrf$^{fl/wt}$ mice (*P=0.028*). Two-way ANOVA followed by Tukey's *post hoc* test to determine individual group differences for **c**, **g**, **h** and **i**. *n*=4-5 mice per group per timepoint. Scale bars are 50µm in **a**, 20 µm in **b** and 5 µm in **d**, **e**, and **f**

Fig. 5 *Myrf* deletion from OPCs does not induce overt demyelination, astrogliosis or inflammation but reduces the number of new oligodendroctyes in the healthy brain two weeks following tamoxifen injection. P-Myrf$^{fl/wt}$ YFP and P-Myrf$^{fl/fl}$ YFP mice were examined on the contralateral side of the corpus callosum (CC) to the lysolecithin lesion 14 DPL. Representative photomicrographs of staining with **a, a'** MBP, **b, b'** GSTπ, **c, c'** GFAP and **d, d'** Iba1. Enlarged images of **e, e'** MBP, **f, f'** GSTπ, **g, g'** GFAP and **h, h'** Iba1. **i** Single merged confocal optical section in the corpus callosum contralateral to lysolecithin lesion in P-Myrf$^{fl/wt}$ mice 14 DPL demonstrating occasional YFP+GSTπ+ oligodendrocytes (arrowhead). Single channel micrograph showing **i'** YFP and **i"** GSTπ. **j** Single merged optical section in the corpus callosum contralateral to the lysolecithin lesion of P-Myrf$^{fl/wt}$ mice 14 DPL demonstrating co-labelling between YFP and PDGFRα (arrowheads). Arrows indicate PDGFRα+ cells which did not recombine (YFP-). Single channel image showing **j'** YFP and **j"** PDGFRα. Quantification showing no difference in cell density of **k** (GSTπ+) and **l** (PDGFRα+) cells in the contralateral side of the corpus callosum between P-Myrf$^{fl/wt}$ and P-Myrf$^{fl/fl}$ mice. **m** Quantification demonstrating recombined cells are unable to differentiate into CNP+ (*P=0.027*) or GSTπ+ (*P=0.032*) oligodendrocytes and a greater percentage remain PDGFRα+ (*P=0.016*) in P-Myrf$^{fl/fl}$ YFP relative to P-Myrf$^{fl/wt}$ YFP mice. Student's T-Test in **k** and **l** and Mann Whitney U Test in **m**, *n*=4-5 mice per group. Scale bars are 100µm in (**a-d**) and (**a'-d'**) and 20µm in (**e-h**),(**e**'-**h**'), **i**, **i'**, **i''** and **j**, **j'**, **j''**

Fig. 6 *Myrf* deletion from OPCs inhibits remyelination. **a** Schematic demonstrating the location of lysolecithin injections into the dorsal column of the C4 spinal cord and location of semi-thin and electron micrographs. **b** Semithin sections at the C4 spinal cord level stained with toluidine blue from P-Myrf$^{fl/wt}$ and P-Myrf$^{fl/fl}$ mice. There are few myelinated axons in P-Myrf$^{fl/fl}$ mice. **c** Electron micrographs of the uninjured and 14 DPL C4 spinal cord in P-Myrf$^{fl/wt}$ and P-Myrf$^{fl/fl}$ mice. **d** Ranking analysis in P-Myrf$^{fl/fl}$ and P-Myrf$^{fl/wt}$ mice, demonstrates there is less remyelination in P-Myrf$^{fl/fl}$ mice (*P=0.030)*. **e** Quantification of the volume of spared tissue that is MBP-negative within the corpus callosum. At 14 DPL, there is a reduction in the MBP-negative volume in P-Myrf$^{fl/wt}$ YFP relative to P-Myrf$^{fl/fl}$ YFP mice (P=0.028). **f** Overview of lesion epicentre in the corpus callosum stained with MBP at 3, 7, and 14 DPL in P-Myrf$^{fl/wt}$ YFP and P-Myrf$^{fl/fl}$ YFP mice. MBP is expressed throughout the corpus callosum at 14 DPL in P-Myrf$^{fl/wt}$ YFP in contrast to P-Myrf$^{fl/fl}$ YFP mice. **g** Quantifications indicating node of Ranvier density in the corpus callosum is reduced (*P=0.047*) but **h** SMI312+ axon staining does not differ between P-Myrf$^{fl/wt}$ YFP and P-Myrf$^{fl/fl}$ YFP mice at 14 DPL (*P=0.754*) in the corpus callosum. **i** Example micrograph of a subset of lesion demonstrating notably fewer punctate Caspr flanking AnkG, in P-Myrf$^{fl/fl}$ YFP relative to P-Myrf$^{fl/wt}$ YFP mice at 14 DPL. Mann Whitney U Test used in **d**, **e** and **g**, Student's T-test in **h**. *n*=4-6 mice per group per time point. Scale bars are 50µm in **b** and **f**, 20µm **i** and 2 µm in **c**

Fig. 7 New oligodendrocytes are unable to effectively remyelinate in P-Myrf$^{fl/fl}$ mT/mG mice. **a** Schematic of the transgenic lines used and experimental timeline. All mice were perfused 28 DPL. **b** Overview of lysolecithin lesion in the corpus callosum stained for GFP and MBP in P-Myrf$^{fl/wt}$ mT/mG and P-Myrf$^{fl/fl}$ mT/mG mice. **c** Quantification demonstrating reductions in the amount of myelin generated by recombined cells within the lesion (GFP+MBP+) in P-Myrf$^{fl/fl}$ mT/mG relative to P-Myrf$^{fl/wt}$ mice (green bars, Mann Whitney U test, *P=0.006*) but myelin generated by non-recombined cells (GFP-MBP+) does not change (clear portion of bars, T-Test, P=0.236). There is less overall MBP in P-Myrf$^{fl/fl}$ mT/mG mice in the lesion (total of bars, T-Test, P=0.020). *n*=6 mice per group. **d** Single optical section of the corpus callosum with axons in cross section reveals co-labelling of GFP with MBP in P-Myrf$^{fl/wt}$ mT/mG mice but almost no GFP+MBP+ sheaths in P-Myrf$^{fl/fl}$ mT/mG mice. **e** Processes from CC1+GFP+ oligodendrocytes (arrowheads) are seen to align along myelinated fibers and co-label with MBP (yellow) in P-Myrf$^{fl/wt}$ mT/mG mice adjacent to lesion epicentre but CC1+GFP+ cells rarely have processes which co-label with MBP in P-Myrf$^{fl/fl}$ mT/mG mice. **f** Single optical confocal coronal section taken at the C4 level of the spinal cord of P-Myrf$^{fl/wt}$ mT/mG and P-Myrf$^{fl/fl}$ mT/mG mice stained with SMI312, MBP, GFP and CC1. Arrows

indicate GFP+CC1+ cell bodies. **g** Enlarged image of individual oligodendrocyte processes from P-Myrf$^{fl/wt}$ mT/mG mice. Within the lesion, numerous GFP+ process surround axons and co-label with MBP indicative of new myelination. **h** Occasional GFP+CC1+ oligodendrocytes wrap axons in P-Myrf$^{fl/fl}$ mT/mG mice, but rarely express MBP. In **g** and **h** arrowheads demarcate GFP+MBP+ myelin, and arrows indicate GFP+ processes wrapping axons that are MBP-negative. Scale bars are 50µm in **b**,10 µm in **d, e** and **f** and 5µm in **g** and **h**

Fig 8 Successful remyelination in MS lesions is associated with MYRF expression in oligodendrocytes. **a** Micrographs of human MS lesions and NAWM stained with luxol fast blue (LFB). Demyelination is observed in active and chronic active plaques, whereas faint LFB staining is present in shadow plaques. **b** Class II HLA reactivity is perilesional in chronic active plaques, and found throughout the lesion in active plaques. **c** Co-labelling between MYRF and the oligodendrocyte lineage marker Sox10 is seen in NAWM. MYRF is primarily nuclear, as indicated by co-labelling with Hoechst. **d** Single optical confocal section demonstrating MYRF is expressed in CNP+ cells within shadow plaques (arrowheads). Arrows indicate CNP+MYRF-negative cells. **e** Example micrographs of single optical confocal sections in chronic active lesion centres and rims demonstrating MYRF is typically expressed in Sox10+NogoA+ oligodendrocytes (arrowhead). Arrows denote Sox10+NogoA+ cells which lack MYRF. **f** Less Hoechst+Sox10+ cells are observed in the centre of chronic active lesions relative to active lesions (*P=0.042*), chronic active rim (*P<0.001*), shadow plaques (*P=0.026*), NAWM (*P<0.001*), and non-MS (*P<0.001*). **g** Less Hoechst+Sox10+MYRF+ cells in chronic lesion centres compared to all other groups *(active lesions P=0.016, chronic active rim P=0.002, shadow plaques P=0.012, NAWM P<0.001, and non-MS P<0.001*). **h** The percentage of Hoechst+Sox10+ cells that express MYRF is reduced in chronic active lesions relative to shadow plaques (*P=0.041)*, NAWM (*P<0.001*) and non-MS white matter (*P<0.001*). **i** The percentage of Sox10+NogoA+ oligodendrocytes which express MYRF is reduced in chronic active lesion centres relative to NAWM (*P<0.001*), shadow plaques (*P<0.001*), and chronic active rims (*P<0.001*). Horizontal lines with vertical dashes above quantifications in **f-i** indicate all statistically significant *post hoc* tests relative to the group with the larger vertical line. One-way ANOVA followed by Tukey's *post hoc* for **f, g, h, i**. Scale bars are 500 µm in **a** and **b**, 50µm in **c**, 20µm in **d** and 10µm in **e**. * = statistical significance

References

1 Bai CB, Sun S, Roholt A, Benson E, Edberg D, Medicetty S, et al. (2016) A mouse model for testing remyelinating therapies. Exp Neurol 283: 330-340 Doi 10.1016/j.expneurol.2016.06.033

2 Barres BA, Raff MC (1999) Axonal control of oligodendrocyte development. The Journal of cell biology 147: 1123-1128

3 Barres BA, Raff MC (1994) Control of Oligodendrocyte Number in the Developing Rat Optic-Nerve. Neuron 12: 935-942 Doi 10.1016/0896-6273(94)90305-0

4 Bo L, Mork S, Kong PA, Nyland H, Pardo CA, Trapp BD (1994) Detection of MHC class II-antigens on macrophages and microglia, but not on astrocytes and endothelia in active multiple sclerosis lesions. Journal of neuroimmunology 51: 135-146

5 Bujalka H, Koenning M, Jackson S, Perreau VM, Pope B, Hay CM, et al. (2013) MYRF Is a Membrane-Associated Transcription Factor That Autoproteolytically Cleaves to Directly Activate Myelin Genes. PLoS biology 11: Doi 10.1371/journal.pbio.1001625

6 Cahoy JD, Emery B, Kaushal A, Foo LC, Zamanian JL, Christopherson KS, et al. (2008) A transcriptome database for astrocytes, neurons, and oligodendrocytes: a new resource for understanding brain development and function. J Neurosci 28: 264-278 Doi 10.1523/JNEUROSCI.4178-07.2008

7 Chang A, Tourtellotte WW, Rudick R, Trapp BD (2002) Premyelinating oligodendrocytes in chronic lesions of multiple sclerosis. The New England journal of medicine 346: 165-173 Doi 10.1056/NEJMoa010994

8 Charles P, Hernandez MP, Stankoff B, Aigrot MS, Colin C, Rougon G, et al. (2000) Negative regulation of central nervous system myelination by polysialylated-neural cell adhesion molecule. Proc Natl Acad Sci U S A 97: 7585-7590 Doi 10.1073/pnas.100076197

9 Denk F, Ramer LM, Erskine EL, Nassar MA, Bogdanov Y, Signore M, et al. (2015) Tamoxifen induces cellular stress in the nervous system by inhibiting cholesterol synthesis. Acta neuropathologica communications 3: 74 Doi 10.1186/s40478-015-0255-6

10 Emery B (2010) Transcriptional and post-transcriptional control of CNS myelination. Current opinion in neurobiology 20: 601-607 Doi 10.1016/j.conb.2010.05.005

11 Emery B, Agalliu D, Cahoy JD, Watkins TA, Dugas JC, Mulinyawe SB, et al. (2009) Myelin gene regulatory factor is a critical transcriptional regulator required for CNS myelination. Cell 138: 172-185 Doi 10.1016/j.cell.2009.04.031

12 Fancy SP, Chan JR, Baranzini SE, Franklin RJ, Rowitch DH (2011) Myelin regeneration: a recapitulation of development? Annu Rev Neurosci 34: 21-43 Doi 10.1146/annurev-neuro-061010-113629

13 Fancy SP, Harrington EP, Yuen TJ, Silbereis JC, Zhao C, Baranzini SE, et al. (2011) Axin2 as regulatory and therapeutic target in newborn brain injury and remyelination. Nat Neurosci 14: 1009-1016 Doi 10.1038/nn.2855

14 Fancy SP, Kotter MR, Harrington EP, Huang JK, Zhao C, Rowitch DH, et al. (2010) Overcoming remyelination failure in multiple sclerosis and other myelin disorders. Exp Neurol 225: 18-23 Doi 10.1016/j.expneurol.2009.12.020

15 Franklin RJ, Ffrench-Constant C (2008) Remyelination in the CNS: from biology to therapy. Nat Rev Neurosci 9: 839-855 Doi 10.1038/nrn2480

16 Franklin RJ, ffrench-Constant C, Edgar JM, Smith KJ (2012) Neuroprotection and repair in multiple sclerosis. Nature reviews Neurology 8: 624-634 Doi 10.1038/nrneurol.2012.200

17 Franklin RJ, Hinks GL (1999) Understanding CNS remyelination: clues from developmental and regeneration biology. Journal of neuroscience research 58: 207-213

18 Freeman SA, Desmazieres A, Simonnet J, Gatta M, Pfeiffer F, Aigrot MS, et al. (2015) Acceleration of conduction velocity linked to clustering of nodal components precedes myelination. Proc Natl Acad Sci U S A 112: E321-328 Doi 10.1073/pnas.1419099112

19 Frischer JM, Bramow S, Dal-Bianco A, Lucchinetti CF, Rauschka H, Schmidbauer M, et al. (2009) The relation between inflammation and neurodegeneration in multiple sclerosis brains. Brain 132: 1175-1189 Doi 10.1093/brain/awp070

20 Frischer JM, Weigand SD, Guo Y, Kale N, Parisi JE, Pirko I, et al. (2015) Clinical and pathological insights into the dynamic nature of the white matter multiple sclerosis plaque. Annals of neurology 78: 710-721 Doi 10.1002/ana.24497

21 Gautier HO, Evans KA, Volbracht K, James R, Sitnikov S, Lundgaard I, et al. (2015) Neuronal activity regulates remyelination via glutamate signalling to oligodendrocyte progenitors. Nat Commun 6: 8518 Doi 10.1038/ncomms9518

22 Gonzalez GA, Hofer MP, Syed YA, Amaral AI, Rundle J, Rahman S, et al. (2016) Tamoxifen accelerates the repair of demyelinated lesions in the central nervous system. Sci Rep 6: 31599 Doi 10.1038/srep31599

23 Griffiths I, Klugmann M, Anderson T, Yool D, Thomson C, Schwab MH, et al. (1998) Axonal swellings and degeneration in mice lacking the major proteolipid of myelin. Science 280: 1610-1613

24 Hines JH, Ravanelli AM, Schwindt R, Scott EK, Appel B (2015) Neuronal activity biases axon selection for myelination in vivo. Nat Neurosci 18: 683-689 Doi 10.1038/nn.3992

25 Hornig J, Frob F, Vogl MR, Hermans-Borgmeyer I, Tamm ER, Wegner M (2013) The transcription factors Sox10 and Myrf define an essential regulatory network module in differentiating oligodendrocytes. PLoS genetics 9: e1003907 Doi 10.1371/journal.pgen.1003907

26 Irvine KA, Blakemore WF (2008) Remyelination protects axons from demyelination-associated axon degeneration. Brain 131: 1464-1477 Doi 10.1093/brain/awn080

27 Ishii A, Furusho M, Dupree JL, Bansal R (2014) Role of ERK1/2 MAPK signaling in the maintenance of myelin and axonal integrity in the adult CNS. J Neurosci 34: 16031-16045 Doi 10.1523/JNEUROSCI.3360-14.2014

28 Jeffries MA, Urbanek K, Torres L, Wendell SG, Rubio ME, Fyffe-Maricich SL (2016) ERK1/2 Activation in Preexisting Oligodendrocytes of Adult Mice Drives New Myelin Synthesis and Enhanced CNS Function. J Neurosci 36: 9186-9200 Doi 10.1523/JNEUROSCI.1444-16.2016

29 Kang SH, Fukaya M, Yang JK, Rothstein JD, Bergles DE (2010) NG2+ CNS glial progenitors remain committed to the oligodendrocyte lineage in postnatal life and following neurodegeneration. Neuron 68: 668-681 Doi 10.1016/j.neuron.2010.09.009

30 Keough MB, Rogers JA, Zhang P, Jensen SK, Stephenson EL, Chen T, et al. (2016) An inhibitor of chondroitin sulfate proteoglycan synthesis promotes central nervous system remyelination. Nat Commun 7: 11312 Doi 10.1038/ncomms11312

31 Koenning M, Jackson S, Hay CM, Faux C, Kilpatrick TJ, Willingham M, et al. (2012) Myelin gene regulatory factor is required for maintenance of myelin and mature oligodendrocyte identity in the adult CNS. J Neurosci 32: 12528-12542 Doi 10.1523/JNEUROSCI.1069-12.2012

32 Kornek B, Storch MK, Weissert R, Wallstroem E, Stefferl A, Olsson T, et al. (2000) Multiple sclerosis and chronic autoimmune encephalomyelitis: a comparative quantitative study of axonal injury in active, inactive, and remyelinated lesions. Am J Pathol 157: 267-276 Doi 10.1016/S0002-9440(10)64537-3

33 Kotter MR, Li WW, Zhao C, Franklin RJ (2006) Myelin impairs CNS remyelination by inhibiting oligodendrocyte precursor cell differentiation. J Neurosci 26: 328-332 Doi 10.1523/JNEUROSCI.2615-05.2006

34 Kuhlmann T, Miron V, Cuo Q, Wegner C, Antel J, Bruck W (2008) Differentiation block of oligodendroglial progenitor cells as a cause for remyelination failure in chronic multiple sclerosis. Brain 131: 1749-1758 Doi 10.1093/brain/awn096

35 Kuhlmann T, Remington L, Maruschak B, Owens T, Bruck W (2007) Nogo-A is a reliable oligodendroglial marker in adult human and mouse CNS and in demyelinated lesions. J Neuropath Exp Neur 66: 238-246
36 Kutzelnigg A, Lucchinetti CF, Stadelmann C, Bruck W, Rauschka H, Bergmann M, et al. (2005) Cortical demyelination and diffuse white matter injury in multiple sclerosis. Brain 128: 2705-2712 Doi 10.1093/brain/awh641
37 Lappe-Siefke C, Goebbels S, Gravel M, Nicksch E, Lee J, Braun PE, et al. (2003) Disruption of Cnp1 uncouples oligodendroglial functions in axonal support and myelination. Nature genetics 33: 366-374 Doi 10.1038/ng1095
38 Livak KJ, Schmittgen TD (2001) Analysis of relative gene expression data using real-time quantitative PCR and the 2(T)(-Delta Delta C) method. Methods 25: 402-408 Doi 10.1006/meth.2001.1262
39 Mathis C, Denisenko-Nehrbass N, Girault JA, Borrelli E (2001) Essential role of oligodendrocytes in the formation and maintenance of central nervous system nodal regions. Development 128: 4881-4890
40 McKenzie IA, Ohayon D, Li H, de Faria JP, Emery B, Tohyama K, et al. (2014) Motor skill learning requires active central myelination. Science 346: 318-322 Doi 10.1126/science.1254960
41 Miron VE, Boyd A, Zhao JW, Yuen TJ, Ruckh JM, Shadrach JL, et al. (2013) M2 microglia and macrophages drive oligodendrocyte differentiation during CNS remyelination. Nat Neurosci 16: 1211-1218 Doi 10.1038/nn.3469
42 Muzumdar MD, Tasic B, Miyamichi K, Li L, Luo L (2007) A global double-fluorescent Cre reporter mouse. Genesis 45: 593-605 Doi 10.1002/dvg.20335
43 Najm FJ, Madhavan M, Zaremba A, Shick E, Karl RT, Factor DC, et al. (2015) Drug-based modulation of endogenous stem cells promotes functional remyelination in vivo. Nature 522: 216-220 Doi 10.1038/nature14335
44 Nave KA (2010) Myelination and support of axonal integrity by glia. Nature 468: 244-252 Doi 10.1038/nature09614
45 Nguyen T, Mehta NR, Conant K, Kim KJ, Jones M, Calabresi PA, et al. (2009) Axonal protective effects of the myelin-associated glycoprotein. J Neurosci 29: 630-637 Doi 10.1523/JNEUROSCI.5204-08.2009
46 Patrikios P, Stadelmann C, Kutzelnigg A, Rauschka H, Schmidbauer M, Laursen H, et al. (2006) Remyelination is extensive in a subset of multiple sclerosis patients. Brain 129: 3165-3172 Doi 10.1093/Brain/Awl217
47 Piaton G, Aigrot MS, Williams A, Moyon S, Tepavcevic V, Moutkine I, et al. (2011) Class 3 semaphorins influence oligodendrocyte precursor recruitment and remyelination in adult central nervous system. Brain 134: 1156-1167 Doi 10.1093/brain/awr022
48 Plemel JR, Manesh SB, Sparling JS, Tetzlaff W (2013) Myelin inhibits oligodendroglial maturation and regulates oligodendrocytic transcription factor expression. Glia 61: 1471-1487 Doi 10.1002/Glia.22535
49 Prineas JW, Barnard RO, Kwon EE, Sharer LR, Cho ES (1993) Multiple sclerosis: remyelination of nascent lesions. Annals of neurology 33: 137-151 Doi 10.1002/ana.410330203
50 Prineas JW, Kwon EE, Goldenberg PZ, Ilyas AA, Quarles RH, Benjamins JA, et al. (1989) Multiple sclerosis. Oligodendrocyte proliferation and differentiation in fresh lesions. Laboratory investigation; a journal of technical methods and pathology 61: 489-503
51 Raine CS, Wu E (1993) Multiple sclerosis: remyelination in acute lesions. J Neuropathol Exp Neurol 52: 199-204

52 Rivers LE, Young KM, Rizzi M, Jamen F, Psachoulia K, Wade A, et al. (2008) PDGFRA/NG2 glia generate myelinating oligodendrocytes and piriform projection neurons in adult mice. Nat Neurosci 11: 1392-1401 Doi 10.1038/nn.2220

53 Schneider S, Gruart A, Grade S, Zhang Y, Kroger S, Kirchhoff F, et al. (2016) Decrease in newly generated oligodendrocytes leads to motor dysfunctions and changed myelin structures that can be rescued by transplanted cells. Glia 64: 2201-2218 Doi 10.1002/glia.23055

54 Scholzen T, Gerdes J (2000) The Ki-67 protein: from the known and the unknown. Journal of cellular physiology 182: 311-322 Doi 10.1002/(SICI)1097-4652(200003)182:3<311::AID-JCP1>3.0.CO;2-9

55 Smith KJ, Blakemore WF, Mcdonald WI (1979) Central Remyelination Restores Secure Conduction. Nature 280: 395-396 Doi 10.1038/280395a0

56 Srinivas S, Watanabe T, Lin CS, William CM, Tanabe Y, Jessell TM, et al. (2001) Cre reporter strains produced by targeted insertion of EYFP and ECFP into the ROSA26 locus. BMC developmental biology 1: 4 Doi 10.1186/1471-213X-1-4

57 Stoffels JM, de Jonge JC, Stancic M, Nomden A, van Strien ME, Ma D, et al. (2013) Fibronectin aggregation in multiple sclerosis lesions impairs remyelination. Brain 136: 116-131 Doi 10.1093/brain/aws313

58 Stolt CC, Rehberg S, Ader M, Lommes P, Riethmacher D, Schachner M, et al. (2002) Terminal differentiation of myelin-forming oligodendrocytes depends on the transcription factor Sox10. Genes & development 16: 165-170 Doi 10.1101/gad.215802

59 van der Valk P, De Groot CJ (2000) Staging of multiple sclerosis (MS) lesions: pathology of the time frame of MS. Neuropathology and applied neurobiology 26: 2-10

60 Wingerchuk DM, Weinshenker BG (2000) Multiple sclerosis: epidemiology, genetics, classification, natural history, and clinical outcome measures. Neuroimaging Clin N Am 10: 611-624 ,vii

61 Wolswijk G (2002) Oligodendrocyte precursor cells in the demyelinated multiple sclerosis spinal cord. Brain 125: 338-349

62 Wolswijk G (2000) Oligodendrocyte survival, loss and birth in lesions of chronic-stage multiple sclerosis. Brain 123 (Pt 1): 105-115

63 Xiao L, Ohayon D, McKenzie IA, Sinclair-Wilson A, Wright JL, Fudge AD, et al. (2016) Rapid production of new oligodendrocytes is required in the earliest stages of motor-skill learning. Nat Neurosci 19: 1210-1217 Doi 10.1038/nn.4351

64 Yeung MSY, Zdunek S, Bergmann O, Bernard S, Salehpour M, Alkass K, et al. (2014) Dynamics of Oligodendrocyte Generation and Myelination in the Human Brain. Cell 159: 766-774 Doi 10.1016/j.cell.2014.10.011

Fig1

Click here to download figure Fig1.tif

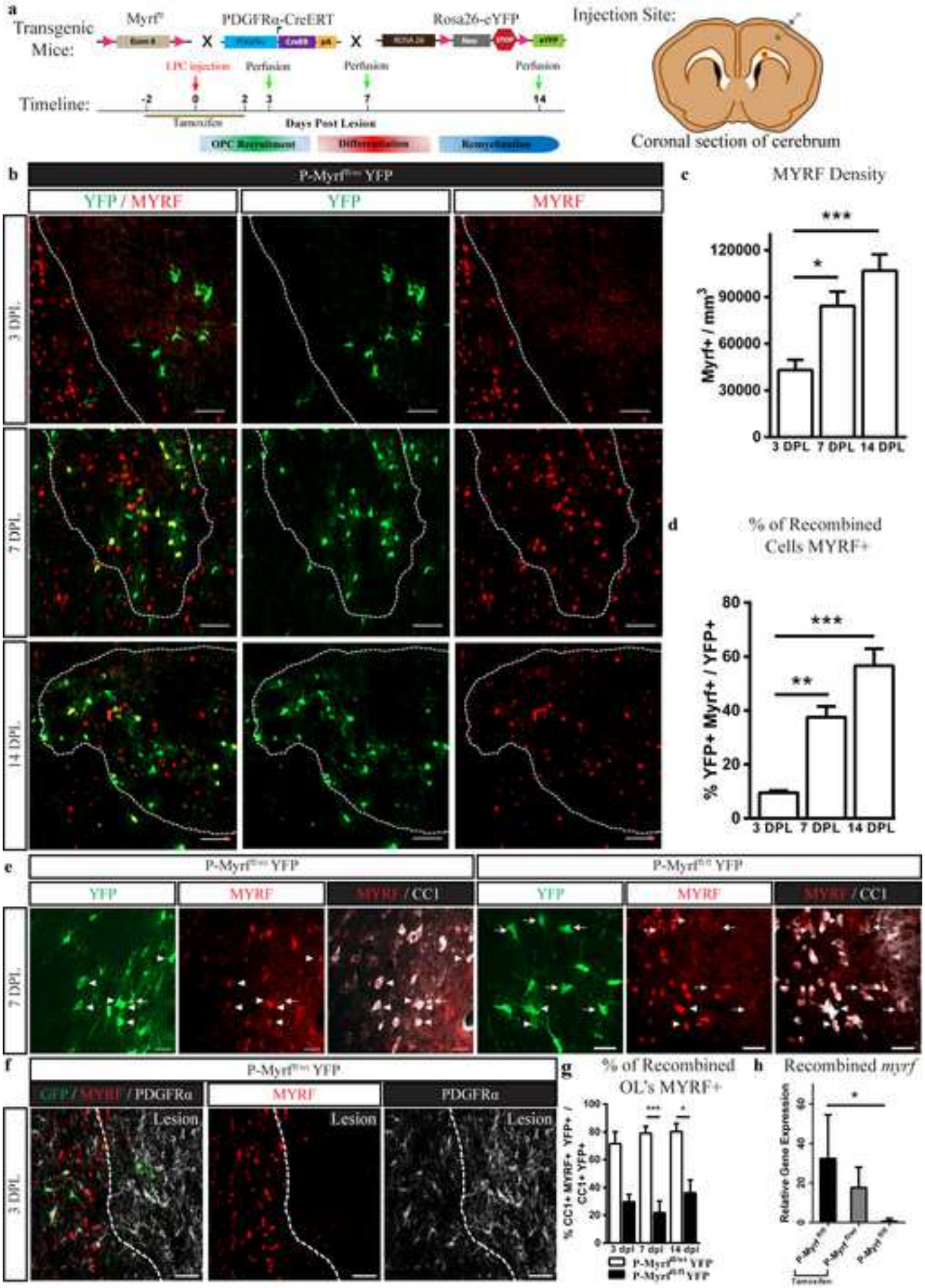

Fig2

Click here to download figure Fig2.tif

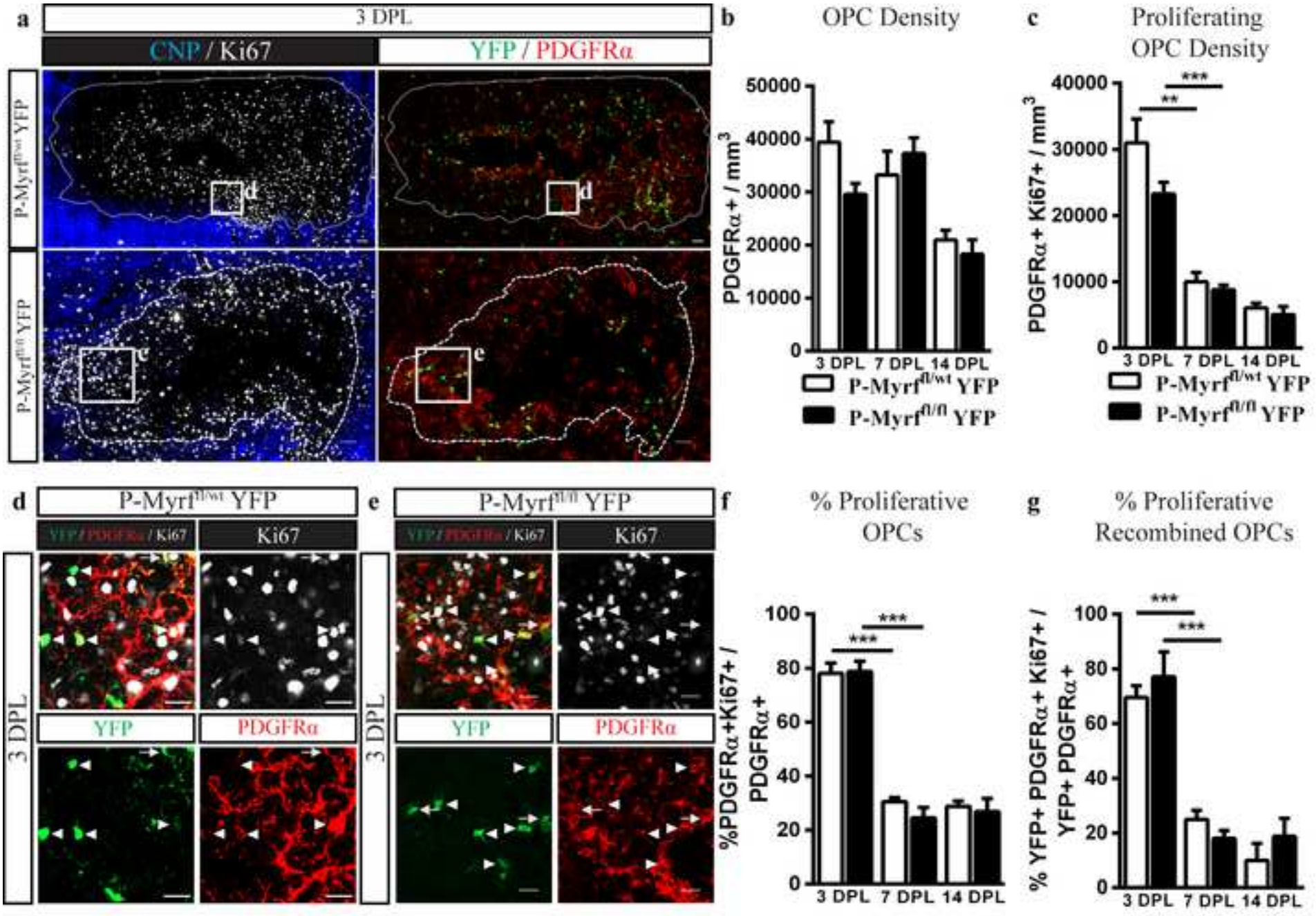

Fig3

Click here to download figure Fig3.tif

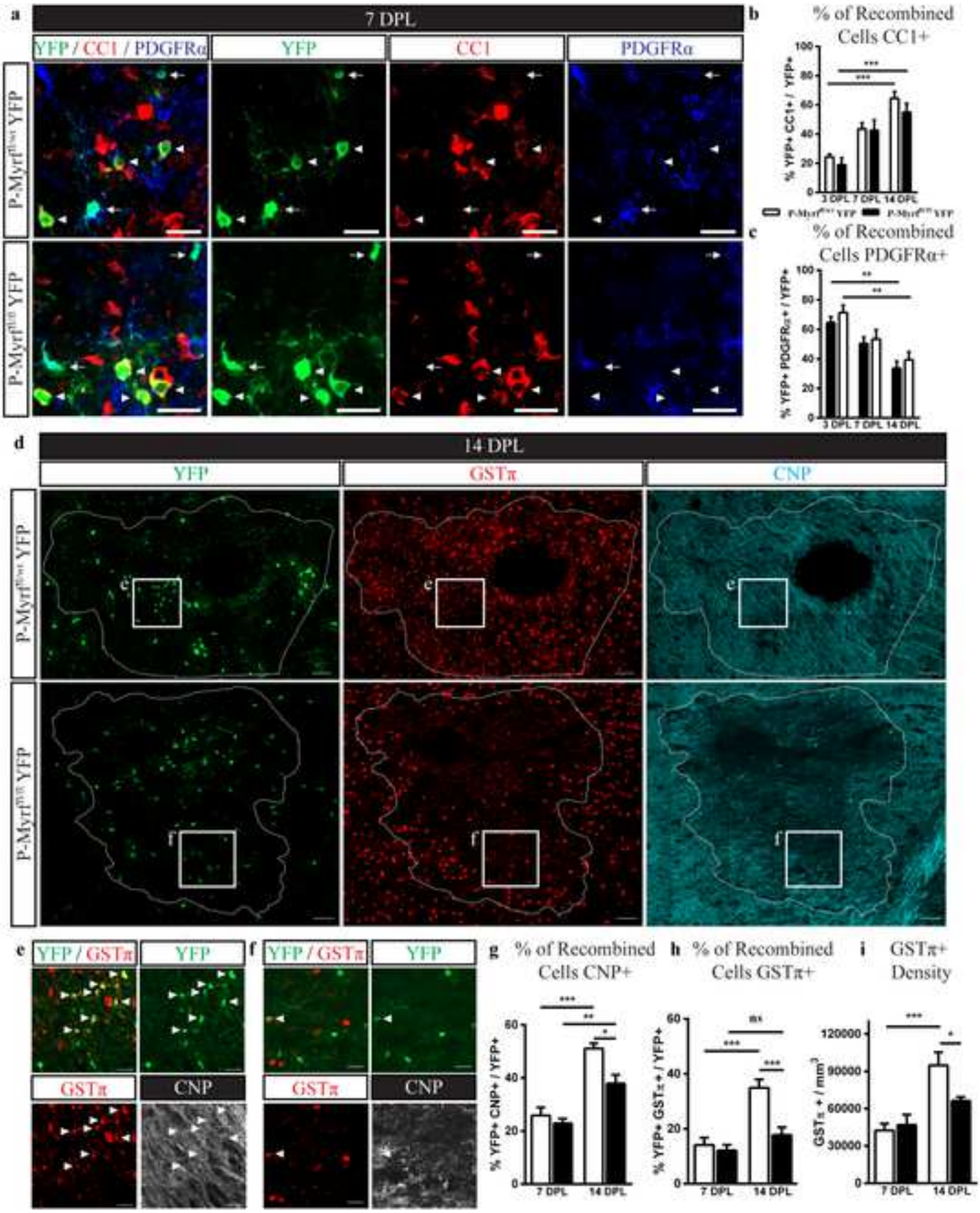

Fig4

Click here to download figure Fig4.tif

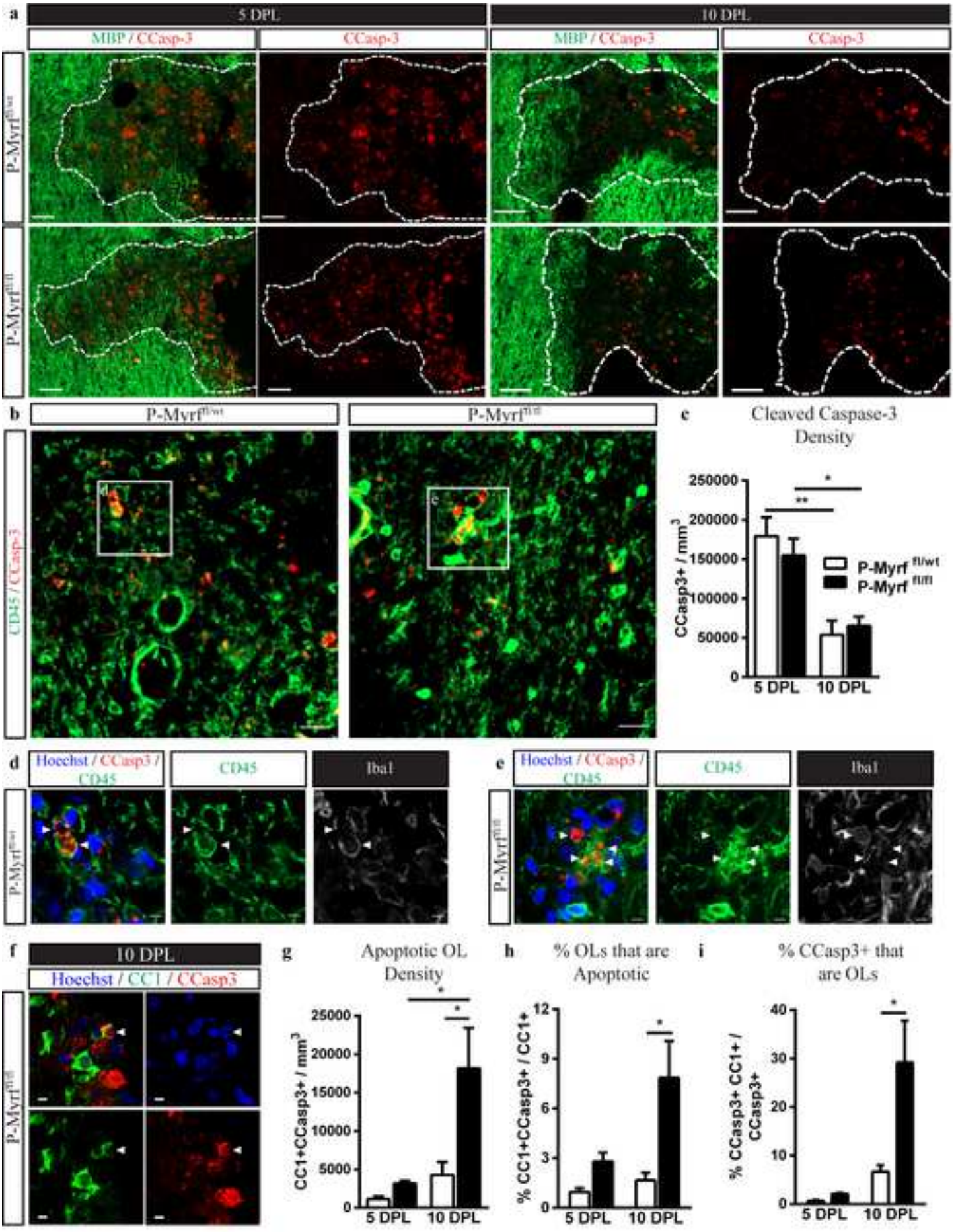

Fig5

Click here to download figure Fig5.tif

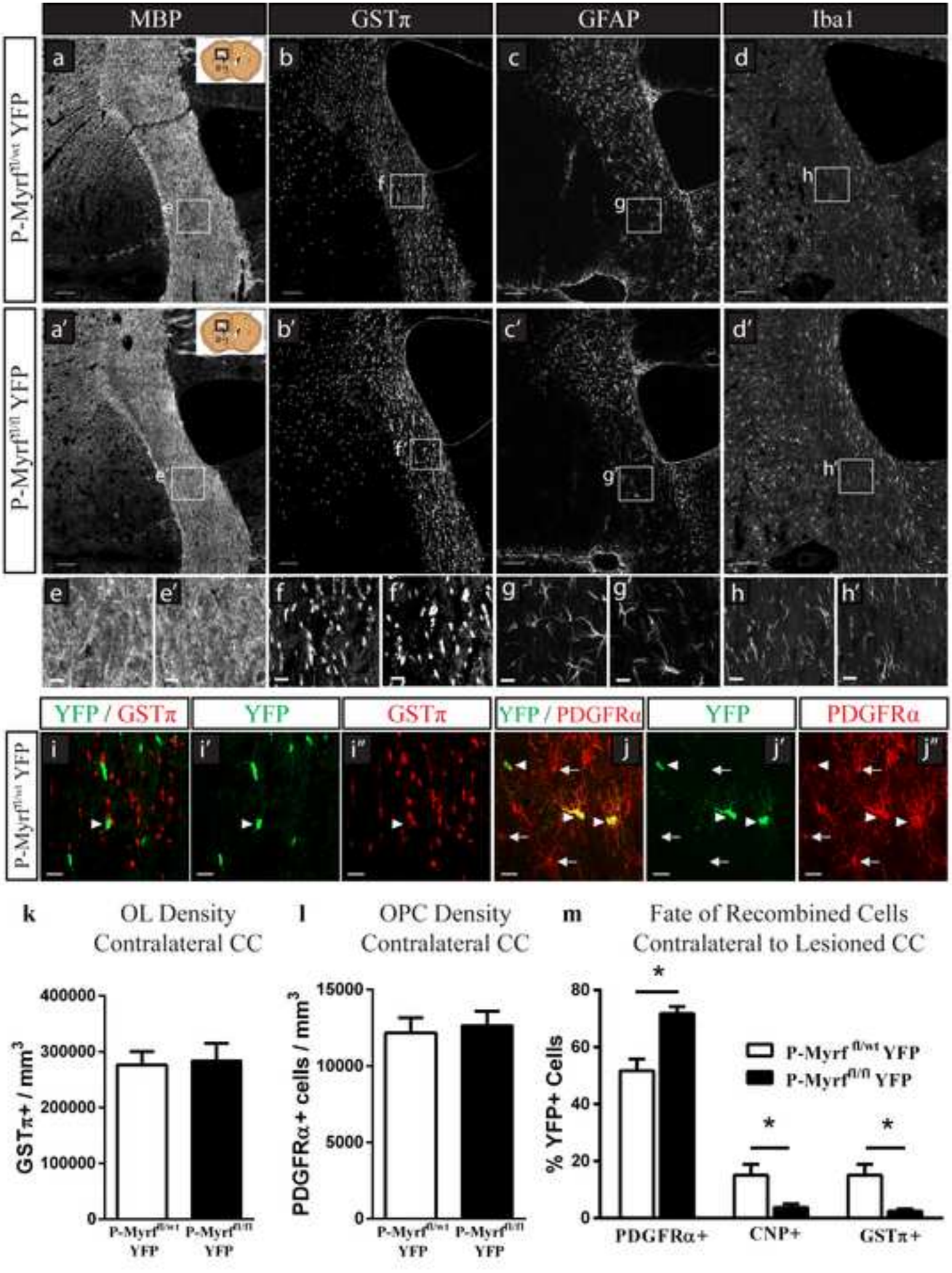

Click here to download figure Fig6.tif

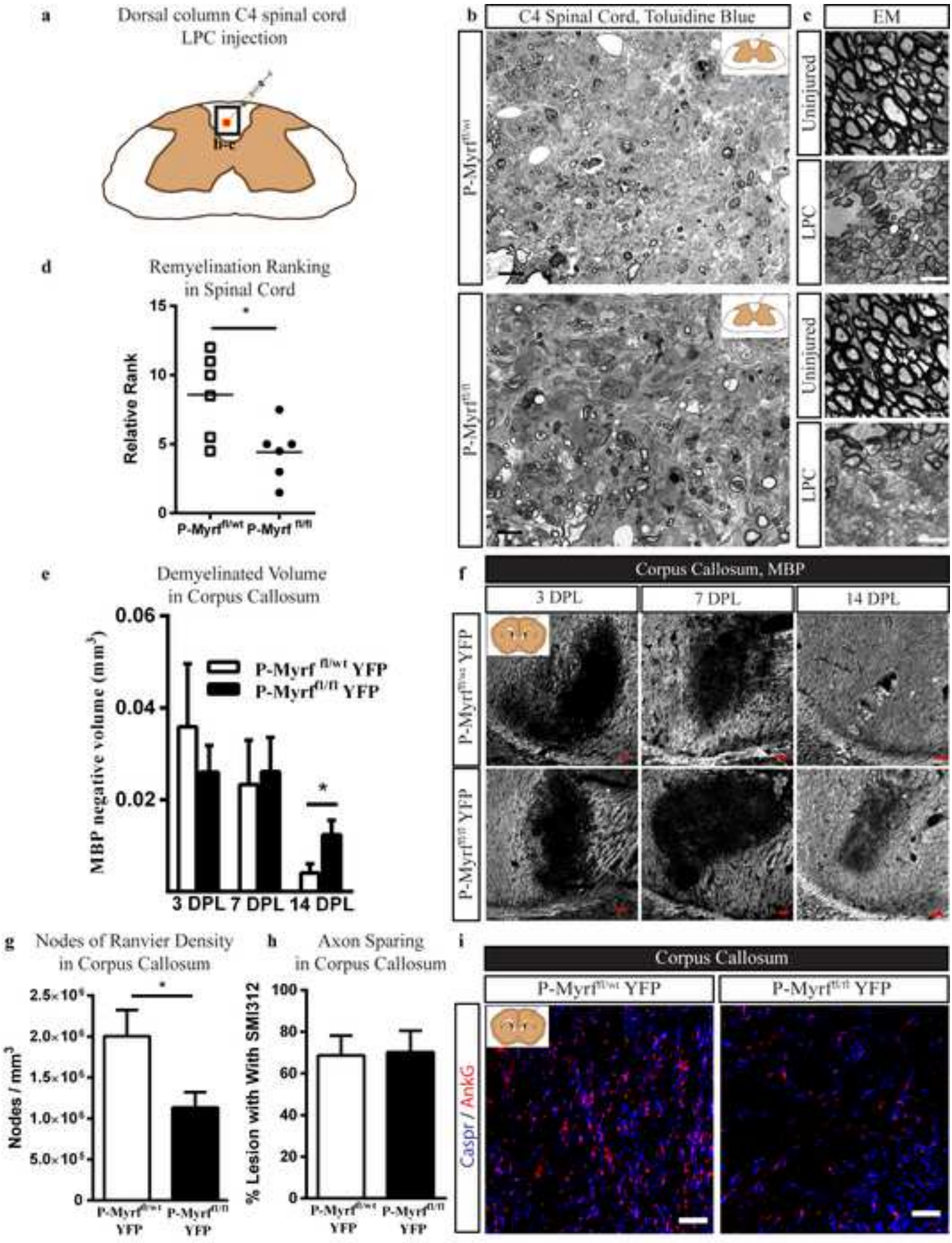

Fig7

Click here to download figure Fig7.tif

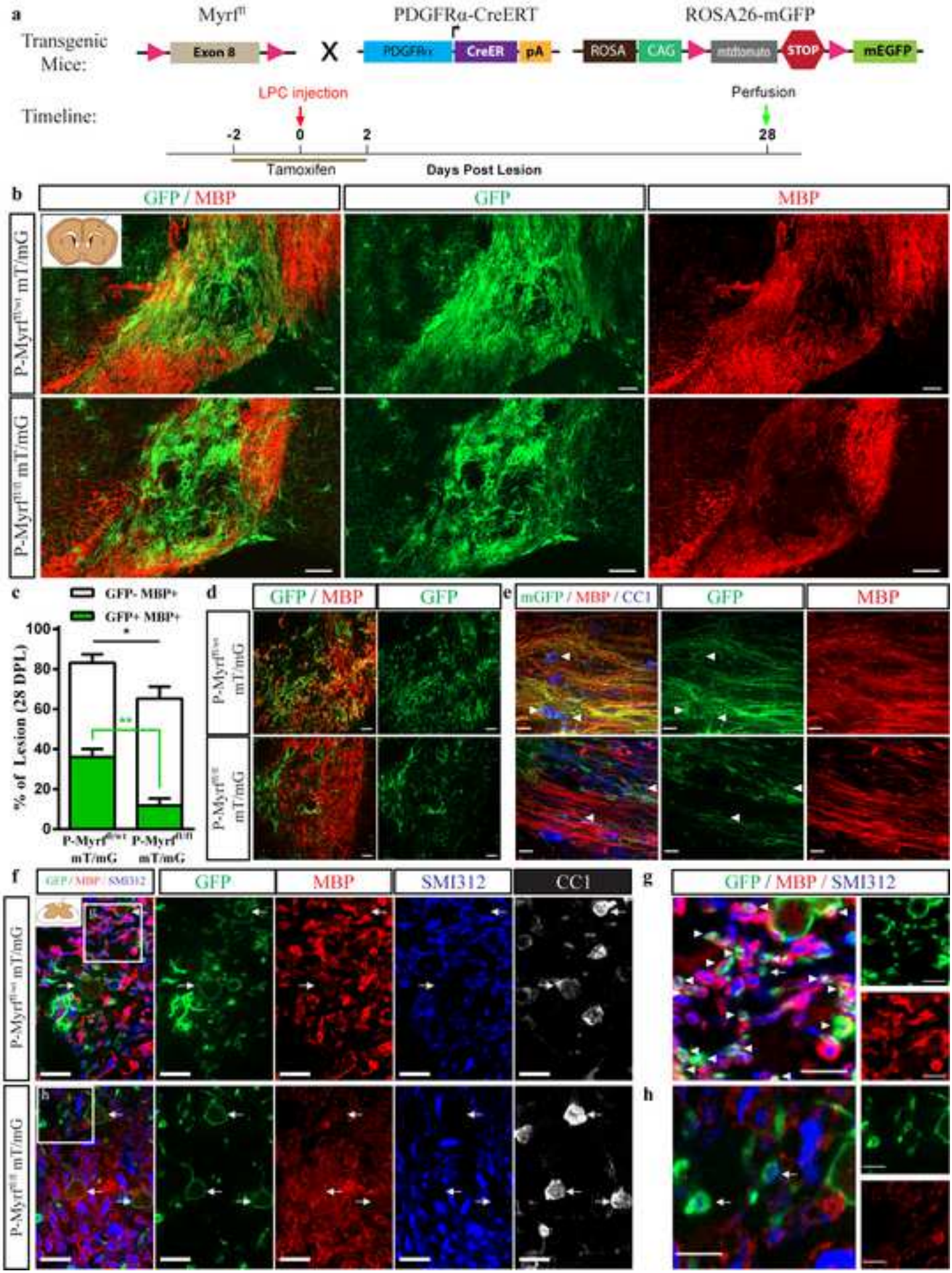

Fig8

Click here to download figure Fig8.tif